LICENTIATE THESIS

Preparation and Properties of Dried Nanofibrillated Cellulose and its Nanocomposites

Christian Eyholzer

LULEÅ UNIVERSITY OF TECHNOLOGY

LULEÅ UNIVERSITY OF TECHNOLOGY

Preparation and properties of dried nanofibrillated cellulose and its nanocomposites

Christian Eyholzer

Luleå University of Technology

Department of Applied Physics and Mechanical Engineering

Division of Wood and Bionanocomposites

SE-971 87 LULEÅ

Sweden

Empa, Swiss Federal Laboratories for Materials Science and Technology

Department of Civil and Mechanical Engineering

Wood Laboratory

CH-8600 DÜBENDORF

Switzerland

May 2010

EMPA

Materials Science & Technology

Printed by Universitetstryckeriet, Luleå 2010

ISSN: 1402-1757
ISBN 978-91-7439-116-9

Luleå 2010

www.ltu.se

Meinen Eltern Ruth und Beat
Meinen Geschwistern Janine und René
Und meiner Frau Anita

Abstract

During the past decade there has been a growing interest in the reinforcement of synthetic polymers by cellulose fibres or fibre fragments. Some work has already been carried out on cellulose nanowhiskers and nanofibrils obtained from plants or animals. These whiskers or fibrils have been used as reinforcement components in synthetic polymers for the production of films and lacquer. Depending on the proportion of cellulose, the composites have shown improved mechanical properties.

The production of fully degradable nanocomposites with biopolymers as matrix and cellulose nanofibrils with high aspect ratios as reinforcement is still a challenging task. Also, due to the large amount of hydroxyl groups on the surface of these nanofibrils, they tend to irreversibly agglomerate during drying. This process, known as hornification, decreases the aspect ratio of the nanofibrils. Consequently, their reinforcing potential in nanocomposites is lowered. Thus, the objective of this PhD project is to produce novel biopolymer composites that are reinforced by functionalised cellulose nanofibrils in powder form. A successful preparation of such bio-based composites could open up ways to new applications in e.g. medicine, bio-packaging or horticulture. In order to induce an optimal compounding of the fibrils with different biopolymers, good fibril/matrix embedding is required. Therefore, the cellulose nanofibrils have to be modified appropriately to match the hydrophilic or hydrophobic nature of the polymer matrix.

In the first study, water-redispersible, nanofibrillated cellulose (NFC) in powder form was prepared from refined, bleached beech pulp (RBP) by carboxymethylation and mechanical disintegration. The sequence of the treatments influenced the stability of the final products in water. When carboxymethylation was applied first, enhanced disintegration of RBP into its sub-structural elements was observed. The prepared powder of this route formed a stable gel in water without sedimentation after 20 h. SEM images affirmed a significant reduction of cellulose nanofibrils agglomeration compared to unmodified NFC. The results suggest that NFC in dry form could be used as an alternative to conventional NFC in aqueous suspensions used as starting material for derivatization and compounding with biopolymers.

The second study focused on the characterization of composites containing poly(vinyl acetate) and the above mentioned chemically modified cellulose nanofibrils by dynamic mechanical analysis (DMA). Also, the suitability of using the nanofibrils to formulate PVAc adhesives for wood bonded assemblies was studied. The results showed that the presence of nanofibrillated cellulose had a strong influence on the viscoelastic properties of PVAc latex films. For all nanocomposites, increasing amounts of NFC (treated or untreated) led to increasing reinforcing effects in the glassy state. This reinforcement primarily resulted from interactions between the cellulose fibrils network and the hydrophilic PVOH matrix that led to the complete disappearance of the PVOH glass transition (tan delta peak) for some fibril types and contents. At any given concentration in the PVOH transition, the nanofibrils which were prepared by chemical modification followed by the mechanical disintegration provided the highest reinforcement. Finally, the use of the chemically modified nanofibrils to prepare adhesives for wood bonding was promising; even though they generally performed worse in dry and wet conditions the boards showed superior heat resistance (EN 14257) and passed the test for durability class D1.

In the third study nanocomposites of hydroxypropyl cellulose (HPC) and nanofibrillated cellulose (NFC) were prepared by solution casting. The various NFC were in form of powders and were prepared from refined, bleached beech pulp (RBP) by mechanical disintegration, optionally combined with a pre- or post mechanical carboxymethylation. Dynamic mechanical analysis (DMA) and tensile tests were performed to compare the reinforcing effects of the NFC to those of their never-dried analogues. Carboxymethylated NFC showed the same mechanical properties in HPC, regardless of being dried or not before casting. This suggested that the effect of irreversible agglomeration of the fibrils during drying (hornification) was prevented by the carboxylate groups on the surface of the fibrils. SEM characterization confirmed a homogeneous dispersion of dried, carboxymethylated NFC within the HPC matrix. These results clearly demonstrate that drying of carboxymethylated NFC to a powder does not decrease its reinforcing potential in the (bio)nanocomposites.

All these strategies have in common that the matrix and the dried nanofibrils form a non-covalently bound composite. Using different reactants with various polarities, modified cellulose fibrils compatible with different biopolymer matrices will be presented. A thorough characterization of morphological, physical-chemical and thermal-mechanical properties of the composites completes the research program.

Table of contents

Abstract **i**

Table of contents **iii**

List of papers **iv**

1 Introduction **1**

1.1 Pulping Processes 1

1.1.1 Mechanical Pulping 1

1.1.2 Chemical Pulping 2

1.2 Cellulose 3

1.2.1 The Structure of Cellulose 3

1.2.2 Nanofibrillated Cellulose 7

1.2.3 Cellulose Whiskers 9

1.3 Lignin 10

1.3.1 The Structure of Lignin 10

1.4 Hemicelluloses 12

1.5 Hornification 14

1.6 Objectives 15

2 Experimental Procedures **16**

2.1 Materials 16

2.2 Mechanical Isolation of NFC 16

2.3 Tests and Analysis 17

3 Summary of appended papers **18**

4 Conclusions **20**

5 Outlook **20**

6 Acknowledgements **21**

7 References **22**

Appended papers

Papers I – III

List of papers

This licentiate thesis is based on reported work of the following papers:

Paper I

Preparation and characterization of water-redispersible nanofibrillated cellulose in powder form

C. Eyholzer, N. Bordeanu, F. Lopez-Suevos, D. Rentsch, T. Zimmermann, K. Oksman

*Cellulose **2010** 17, 19-30*

Paper II

DMA analysis and wood bonding of PVAc latex reinforced with cellulose nanofibrils

F. Lopez-Suevos, C. Eyholzer, N. Bordeanu, K. Richter

*Cellulose **2010**, 17, 387-398*

Paper III

Reinforcing effect of carboxymethylated nanofibrillated cellulose powder on hydroxypropyl cellulose

C. Eyholzer, F. Lopez-Suevos, P. Tingaut, T. Zimmermann, K. Oksman

*Cellulose **2010**, DOI 10.1007/s10570-010-9423-9*

1 Introduction

Nanocomposites can be described as engineered structures from two or more materials with different physical or chemical properties of which one component has at least one dimension in the nanometer scale (below 100nm). Wood is a natural nanocomposite with cellulose fibrils in a matrix of lignin and hemicelluloses. The objectives of this work are the isolation of cellulose fibrils with diameters in the nano scale and their drying to a powder without affecting its structure. Furthermore, nanocomposites with nanofibrillated cellulose and a biopolymer matrix should be prepared.

In this chapter, the basic structure of wood and its main constituents (cellulose, hemicelluloses and lignin) is explained and cellulose fibrils with diameters in the nano scale can be isolated. Finally, the problem of hornification of cellulose upon drying will be explained in the last part.

1.1 Pulping Processes

Pulp consists of cellulose fibers, usually acquired from wood. The liberation of these fibers from the wood matrix can be done in two ways, either mechanically or chemically. Mechanical methods are energy consuming; however they make use of almost the whole wood material. In chemical pulping, only approximately half of the wood becomes pulp, the other half is dissolved. However, modern chemical pulping mills efficiently recover the chemicals and burn the remaining residues. The combustion heat covers the whole energy consumption of the pulp mill (Ek et al. **2009**).

1.1.1 Mechanical Pulping

Groundwood pulp is produced by pressing round wood logs against a rotating cylinder made of sandstone, scraping the fibers off. Another type of mechanical pulp is refiner pulp, obtained by feeding wood chips into the center of rotating, refining discs in the presence of water spray. The disks are grooved, the closer the wood material gets to the edge of the disk, the finer the pulp (Ek et al. **2009**).

Apart from fibers released from the wood matrix, mechanical pulp also contains fines. These are smaller particles, such as broken fibers, giving the mechanical pulp its specific optical characteristics (Sjöström **1993**, Ek et al. **2009**).

1.1.2 Chemical Pulping

The mainly followed strategy to isolate fibers from the wood compartment is to remove the matrix substance lignin. Delignification is done by degrading the lignin molecules, bringing them into solution and removing them by washing. However, there are no chemicals being entirely selective towards lignin. Therefore, also a certain amount of the carbohydrates (cellulose and hemicellulose) is lost in this process. In addition, complete removal of lignin is not possible without severely damaging the carbohydrates. After delignification, some lignin is therefore remaining in the pulp and this amount is determined by the pulp's kappa number. Of all pulp produced worldwide, almost three quarters are chemical pulp, of which the major part is produced by the kraft process (Sjöström **1993**; Ek et al. **2009**).

The kraft process (or sulphate process) is the dominant chemical pulping method worldwide. The cooking chemicals used are sodium hydroxide (NaOH) and sodium sulphide (Na_2S), with OH^- and HS^- as the active anions in the cooking process. The hydrogen sulphide is the main delignifying agent and the hydroxide keeps the lignin fragments in solution. Optionally, only sodium hydroxide can be used as cooking chemical and this process is called *soda cooking* (Sjöström **1993**; Ek et al. **2009**).

The *sulphite process* involves dissolving lignin with sulphurous acid (H_2SO_3) and hydrogen sulphite ions (HSO_3^-) as active anions in the cooking process. More recently developed pulping methods include the use of organic solvents as ethanol, methanol and peracetic acid (CH_3CO_3H) for delignification (Sjöström **1993**; Ek et al. **2009**).

As a final step, the pulp can be bleached, to obtain a whiter product with lower amounts of impurities and improved ageing resistance (yellowing and brittleness resistance). These effects are mainly connected to lignin in chemical pulp. In several stages, different chemicals are used for bleaching, e.g. hydrogen peroxide (H_2O_2), chlorine dioxide (ClO_2), ozone (O_3) or peracetic acid (Sjöström **1993**; Ek et al. **2009**).

Comparing the *kraft process* and the *sulfite process*, there are numerous differences between the final pulps obtained. Sulfite pulps are more readily bleached and are obtained in higher yields. They are also more readily refined and require less power for refinement. On the other hand, paper from Kraft pulps is generally stronger compared to paper from sulfite pulp, even though the degree of polymerization is lower in Kraft pulp cellulose (Young **1994**).

1.2 Cellulose

Cellulose is mainly isolated from wood, but it can also be obtained from other vascular plants like corn or wheat. Other sources of cellulose include various algae (*Valonia*, *Oocystis apiculata*), tunicates and even bacteria (*Gluconacetobacter xylinus*). Depending on the source of cellulose, its structure can vary considerably.

1.2.1 The Structure of Cellulose

Cellulose is composed of polymer chains consisting of unbranched β(1→4) linked D-glucopyranosyl units (anhydroglucose unit, AGU) (Fig. 1.1). The length of these β(1→4) glucan chains depends on the source of cellulose. For wood, a degree of polymerization (DP) of up to 10'000 was found. However, such large chains of insoluble molecules are difficult to measure, due to enzymatic or mechanical degradation during analysis (O'Sullivan **1997**; Klemm et al. **2005**).

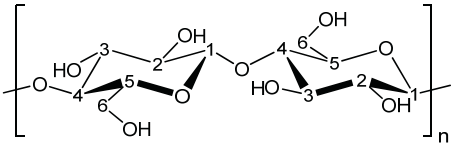

Fig. 1.1 Anhydro-cellobiose unit consisting of two anhydroglucose units (AGU) linked by a β(1→4) glycosidic bond. In this notation, the degree of polymerization (DP) corresponds to n/2.

Three hydroxyl groups, placed at the positions C_2 and C_3 (secondary hydroxyl groups) and C_6 (primary hydroxyl groups) can form intra- and intermolecular hydrogen bonds. These hydrogen bonds allow the creation of highly ordered, three-dimensional crystal structures.

In vascular plants the glucan chains are synthesized in transmembrane protein complexes, called cellulose synthase complex (CSC) or terminal complex (TC). The TC consists of a globule in the center and six hexagonally arranged particles that form a rosette which has a diameter of around 25nm (Fig. 1.2). Freeze-fractured samples of plant cell walls proved the existence of the rosette in the plasmatic face of the plasma membrane (Fig. 1.3 left). In current opinion, each of the six lobes of this rosette consists of six enzymes, the cellulose synthases. The synthases each polymerize a single glucan chain, using uridine diphosphate glucose (UDP-glucose) as a substrate. The individual chains then assemble and crystallize to a single cellulose microfibril (MF) with a diameter of 3.5nm (for wood), by implication consisting of 36 glucan chains (Diotallevi and Mulder **2007**). However, the actual number of active catalytic subunits, defining the number of glucan chains per microfibril has never

been experimentally demonstrated and is still subject of research (Besseuille and Bulone **2008**). In this context it has to be mentioned that the term "microfibril" is a historical term and defines the smallest entity that can be isolated from the cell wall structure. It does not reflect the real nano size of these fibrils which is in the range of 3 to 30nm, depending on the source of the cellulose.

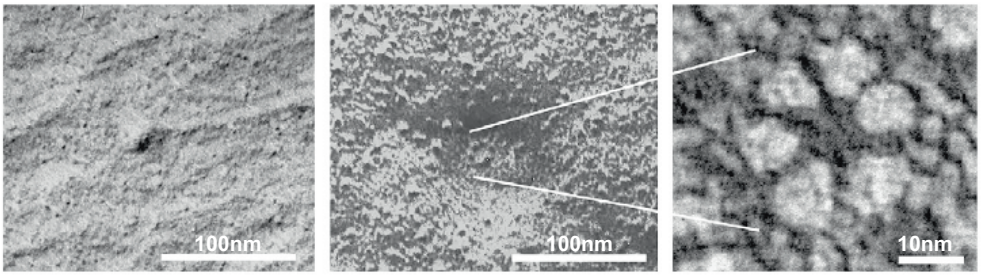

Fig. 1.2 Electron micrographs from freeze-fractured samples of a plant cell wall, showing the imprint of a terminal complex in the exoplasmatic face of the plasma membrane *(left)* the outward-facing side of a TC, the particle-rosette with a characteristic depression of the plasma membrane *(middle)* and a close-up of the particle-rosette with the typical six-folded symmetry *(right)* (Diotallevi and Mulder **2007**).

A second form of terminal complexes was observed in different algae and in the bacterium *Gluconacetobacter xylinus*, showing linear arrays of synthesizing enzymes (Fig. 1.3 right) of varying number, depending on the organism (Delmer **1987**; Besseuille and Bulone **2008**).

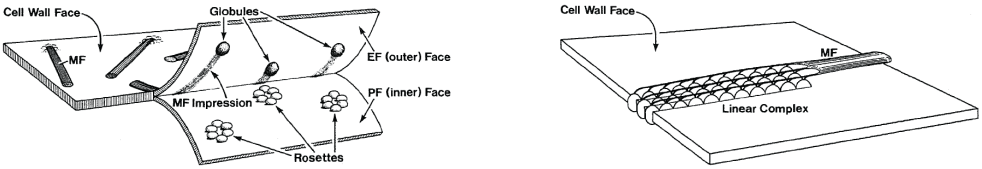

Fig. 1.3 Schematic drawings of terminal complexes observed by freeze-fracture of plasma membranes. Rosettes and globules are found in cellulosic algae and in lower and higher plants. The rosettes fracture with the plasmatic face, while the globules fracture with the exoplasmatic face of the plasma membrane *(left)*. Linear terminal complexes are found in some cellulosic algae and Gluconacetobacter xylinus *(right)*. MF = microfibril (Delmer **1987**).

The biosynthesis of the glucan chains is closely linked to the assembly and crystallization of the glucan chains into highly ordered (crystalline) domains within a microfibril. Native

cellulose (cellulose I) occurs in two different crystalline forms (suballomorphs) designated I_α and I_β, coexisting in variable portions depending on the origin of the cellulose. While cellulose I_α consists of triclinic unit cells the I_β allomorph (which is predominant in higher plants) exhibits a monoclinic type of unit cells. Cellulose II (another allomorph) has been rarely found in nature (e.g. in the marine algae *Halicystis*) but it can be produced artificially from cellulose I by regeneration or mercerization. The regeneration process involves dissolution of the cellulose in a specific solvent (e.g. N-methylmorpholine-N-oxide), while in the mercerization process the cellulose is only swollen in aqueous sodium hydroxide. In both processes, a final re-crystallization step leads to the final cellulose II, which is thermodynamically more stable than the cellulose I allomorph. Interestingly, there has been strong evidence that cellulose II consists of antiparallel chains, opposed to the parallel arrangement of the glucan chains in cellulose I (Besseuille and Bulone **2008**). However, this is still subject of intense discussion. Apart from these structures, there are further allomorphs of cellulose known, namely cellulose III and cellulose IV (Fig. 1.4) (O'Sullivan **1997**; Klemm et al. **2005**).

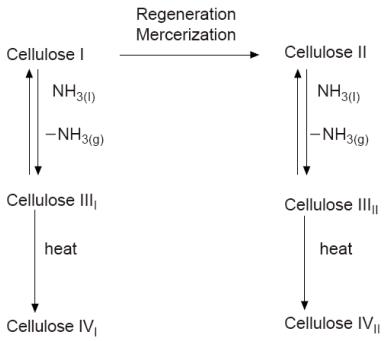

Fig. 1.4 Interconversion of the polymorphs of cellulose (O'Sullivan **1997**).

As illustrated above, the glucan chains of several cellulose synthases assemble and merge into a single microfibril, giving rise to a highly ordered structure. However, these microfibrils are not perfectly crystalline; they also show para-crystalline (amorphous) domains of low order and defects. The generally accepted model is the fringed-fibrillar model, proposing that the single glucan chains pass through an irregular pattern of amorphous and crystalline domains (Fig. 1.5) (Klemm et al. **2005**). During hydrolysis in acidic environment, the glucan chains are preferably cut in the amorphous domains. The resulting microfibril fragments are called whiskers due to their typical slender, rod-like shape.

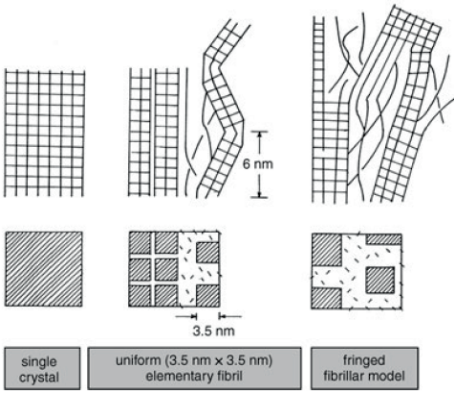

Fig. 1.5 Various models of the structure of single microfibrils (Klemm et al. **2005**).

The single microfibrils then pack to larger bundles (fibril bundles, fibril agglomerates), hold together by the matrix substances (hemicelluloses, lignin and pectin). As the skeletal component in all plants, cellulose is organized in a cellular hierarchical structure. The cell walls of plants are divided by a middle lamella from each other, followed by the primary cell wall layer. The secondary cell wall layer is divided in S1 and S2, with the latter containing the main quantity of cellulose. (Fig. 1.6) (Klemm et al. **2005**).

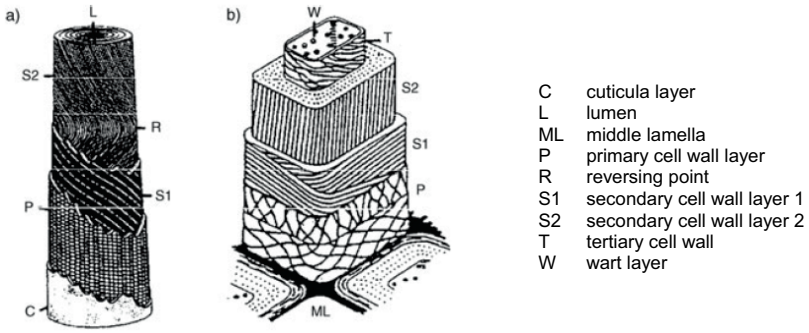

Fig. 1.6 Structural design of plant cell walls exemplified by cotton *(left)* and white fir *(right)* fibers (Klemm et al. **2005**).

The cellulose microfibrils organized in the cell walls have characteristic orientations (microfibril angles), which differ depending on the cell wall layer and according to the plant type. This orientation of the microfibrils is probably directed by microtubules, which have often been found in a parallel orientation to the microfibrils. It is supposed that during the biosynthesis of the glucan chains the TC is driven backwards by the force generated from the rigid microfibrils and that this movement is guided by restriction of lateral movement within channels of oriented microtubules (Delmer **1987**).

The orientation of the microfibrils has a strong effect on the mechanical properties of the fibers of various plant types. For instance, low microfibril angles like in S2 (with microfibril orientation almost parallel to the fiber axis) give rise to a large modulus of elasticity, while large angles lead to higher elongation at break (Klemm et al. **2005**). As a consequence of its fibrillar structure and the large amounts of hydrogen bonds, cellulose has a high tensile strength. It is therefore the structural element of a plant that bears the load in tensile mode (Sjöström **1993**).

1.2.2 Nanofibrillated Cellulose

The first successful isolation of cellulose microfibrils was reported in 1983 (Turbak et al. **1983**; Herrick et al. **1983**). Using a Gaulin laboratory homogenizer, dilute slurries of cut cellulose fibers from softwood pulp were subjected to high shear forces to yield individualized cellulose microfibrils. The resulting gels showed a clear increase in viscosity after several passes through the homogenizer. After carbon dioxide critical point drying of mechanically disintegrated cellulose fibers, scanning electron microscope (SEM) images revealed a network of isolated microfibrils and fibril aggregates (Fig. 1.7).

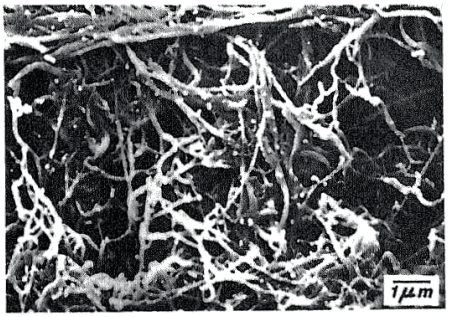

Fig. 1.7 SEM image of softwood pulp after 10 passes through a homogenizer at 55 MPa pressure at a magnification of ca. 10'000x (Herrick et al. **1983**).

As mentioned before, the term microfibril is missleading as it does not reflect the real dimensions of the fibril. Furthermore, it is not possible to obtain a perfectly homogeneous sample of single cellulose microfibrils. Therefore, mechanical disintegration of pulps usually aims at the isolation of cellulose fibril aggregates having diameters below 100nm. In this work, such cellulose portions are termed nanofibrillated cellulose.

Some of the first nanocomposites containing NFC were prepared in 1983 (Boldizar, Klason and Kubát **1983**). Softwood pulp was hydrolyzed in 2.5M hydrochloric acid (HCl) at 105°C and afterwards pumped through a slit homogenizer. By varying the hydrolysis time and the number of passes through the homogenizer several NFC gels were prepared.

These gels were then mixed with poly(vinyl acetate) (PVAc) and films were cast from these suspensions. The authors reported a clear increase in MOE of the nanocomposites (up to 2'900 MPa) compared to the neat PVAc matrix (63 MPa) from tensile tests. In the same work, the NFC was also mixed with a poly(styrene) (PS) matrix. The mixture was then dried to a solid, ground and finally injection molded. However, there was only a rather small reinforcing effect. This was attributed to the drying process of the NFC that reduced its aspect ratio and led to agglomerates within the composites, as observed under the SEM (Boldizar, Klason and Kubát **1983**).

The problem of irreversible agglomeration (or *hornification*) of cellulose upon drying for the preparation of polymer nanocomposites from powder form could not be solved in the following years. Several techniques were suggested, as for instance reaction injection moulding (RIM). In this process, the monomers are proposed to be injected into a mould and polymerized in the presence of the NFC (Zadorecki and Michell **1989**). However, for almost one decade there was little interest in the preparation of nanocomposites from NFC.

In 1998, the preparation of nanocomposites containing NFC and starch as a matrix was reported (Dufresne and Vignon **1998**). Dynamic Mechanical Analysis (DMA) showed that the storage modulus in the rubbery plateau of starch was clearly increased when the polymer was reinforced with NFC. This increase in storage modulus in the rubbery plateau of a thermoplastic matrix upon compounding with NFC was attributed to the formation of a percolating NFC network. This network is created due to a large amount of hydrogen bonds between the isolated fibrils and provides a drastic increase in stiffness of the composite, originating from the rigidity of the network (Dufresne and Vignon **1998**).

Other hydrophilic polymer matrices like poly(vinyl alcohol) (PVOH) or hydroxypropyl cellulose (HPC) were used to prepare nanocomposites containing NFC. Tensile tests showed that both, MOE and tensile strength were significantly increased upon addition of NFC to the polymer matrices (Zimmermann et al. **2004**).

In addition, also hydrophobic polymers, like polyurethane were used as a matrix for the preparation of nanocomposites. In a film-stacking method, thin films of dried NFC and polyurethane were stacked and compression molded. Also for this method, the thermal stability of the composite was clearly increased compared to the neat polyurethane. Again, this was attributed to a percolating network of NFC (Seydibeyoğlu and Oksman **2008**).

In the last few years, research on nanocomposites containing NFC has been noticeably intensified. This development is reflected by a number of detailed reviews, providing a detailed overview on this research topic (Hubbe et al. **2008**; Siró and Plackett **2010**).

1.2.3 Cellulose Whiskers

One of the first reports on nanocomposites containing cellulose whiskers was presented in 1995 (Favier et al. **1995**). Mantles of tunicates (a worm-like sea animal) were cut in small fragments and bleached, followed by a disintegration process using a blender and a Gaulin laboratory homogenizer. The resulting suspension was then hydrolyzed with 55% w/w sulfuric acid (H_2SO_4). SEM images revealed rod-like, highly crystalline cellulose whiskers with diameters and lengths in the nano scale (Fig. 1.8).

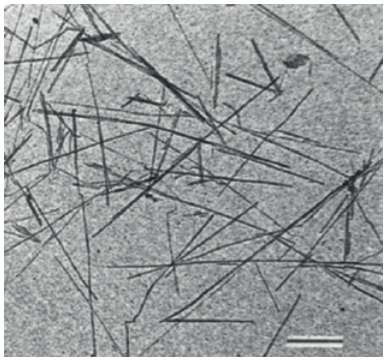

Fig. 1.8 SEM image of rod-like cellulose whiskers from tunicates after a disintegration process, followed by hydrolysis in sulfuric acid (Favier et al. **1995**).

The reinforcing effect of cellulose whiskers was compared to the effect of NFC in a poly(styrene-co-butyl acrylate) latex. It was showed that both fillers led to an increase in tensile modulus and tensile strength. However, the incorporation of NFC resulted in significantly higher values, due to the entanglements between the fibrils leading to a rigid network of NFC. In addition, DMA analysis showed a higher thermal stability (higher storage modulus) in the rubbery state of the polymer latex when reinforced with NFC, compared to whiskers. (Azizi Samir et al. **2004**).

Nanocomposites containing cellulose whiskers and poly(lactic acid) (PLA) were prepared by extrusion. The whiskers were prepared by swelling microcrystalline cellulose in N,N-dimethylacetamide / lithium chloride (DMAc/LiCl), followed by ultrasonication of the suspension. To avoid the problem of aggregation of the whiskers during drying, the suspension was fed directly into the polymer melt during the extrusion process. The vapor generated by feeding the whisker suspension was removed by several venting systems. However, the suspension enhanced thermal degradation of the whiskers. The addition of poly(ethylene glycol) (PEG) improved the dispersion of the whiskers in PLA. However, the nanocomposites did not show improvements in mechanical properties compared to neat PLA. This was mainly attributed to the combination of the used additives (DMAc/LiCl and PEG) (Oksman et al. **2006**).

Another approach to prepare nanocomposites containing cellulose whiskers and PLA comprised the use of a surfactant on the whiskers. The surfactant treated whiskers were freeze-dried and dispersed in chloroform under ultrasonication. Thin films were cast from the mixtures in silicon molds. SEM images showed an increase in the dispersion of the surfactant modified whiskers within the PLA compared to the dispersion of conventional whiskers. In addition, DMA analysis showed an interaction between the PLA matrix and the surfactant modified whiskers due to a shift of the glass temperature (tan δ peak) of 22K (Petersson, Kvien and Oksman **2007**).

In recent years, the number of works on the preparation of nanocomposites containing cellulose whiskers has clearly increased. A more detailed overview on this topic can be obtained from several reviews (Hubbe et al. **2008**; Siró and Plackett **2010**).

1.3 Lignin

The matrix substance lignin can be isolated from extractive-free wood as an insoluble residue after hydrolytic removal of the polysaccharides (cellulose and hemicelluloses). *Klason lignin* is obtained after removing the polysaccharides with 72% sulfuric acid for 2h (primary hydrolysis) and with 3% sulfuric acid under reflux at boiling temperature for 4h (secondary hydrolysis). The drawback of this method is the extensive change in the structure of the lignin. Other methods apply the use of enzymes to remove the polysaccharides. These routes are tedious, but the resulting *cellulolytic enzyme lignin* retains its original structure essentially unchanged (Sjöström **1993**).

1.3.1 The Structure of Lignin

The matrix substances in the natural composite of wood are the lignins. Their basic function in the wood composite is to carry the compression loads acting on the cell walls. Lignins are amorphous polymers of phenylpropane units. In addition to the propane group, the phenyl rings are often substituted with hydroxyl, methoxy, alkoxy or aryloxy groups. In wood, there are typically two main phenylpropane units. *Guaiacyl lignin* occurs in almost all softwoods and is largely a polymerization product of coniferyl alcohol, containing a hydroxyl and a methoxy group at the phenylpropane unit. *Guaiacly-syringyl lignin*, typical for hardwoods, is a copolymer of coniferyl and sinapyl alcohols. The syringyl lignin contains a hydroxyl and two methoxy groups. Finally, compression wood has a high proportion of p-hydroxyphenyl units in addition to the guaiacyl units (Fig. 1.9) (Sjöström **1993**).

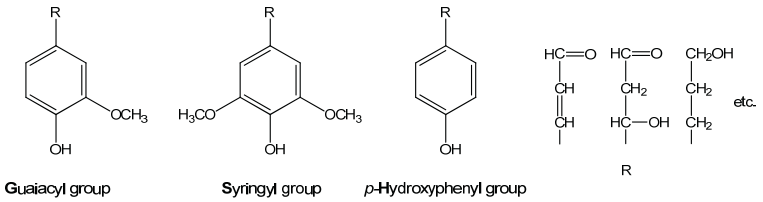

Fig. 1.9 The two main components of lignin in wood, the guaiacyl group in softwood *(left)* and the syringyl group (co-polymerized with guaiacyl groups) in hardwood *(middle left)* and the p-hydroxyphenyl group in compression wood *(middle right)*. The propane groups can have various hydroxyl, ketone or aldehyde groups *(right)* (Sjöström **1993**).

Only relatively few of the phenolic hydroxyl groups are free, most of them are occupied through linkages to neighboring phenylpropane units. Especially the syringyl units in hardwood lignin are extensively etherified. However, there are large individual variations among the wood species concerning the ether and ester linkages in lignin. Even within the cell walls, the composition of lignin varies. In an attempt to illustrate a general structure of lignin, Adler's formula represents a segment of a lignin macromolecule with some examples of typical phenylpropane units (Fig. 1.10) (Sjöström **1993**).

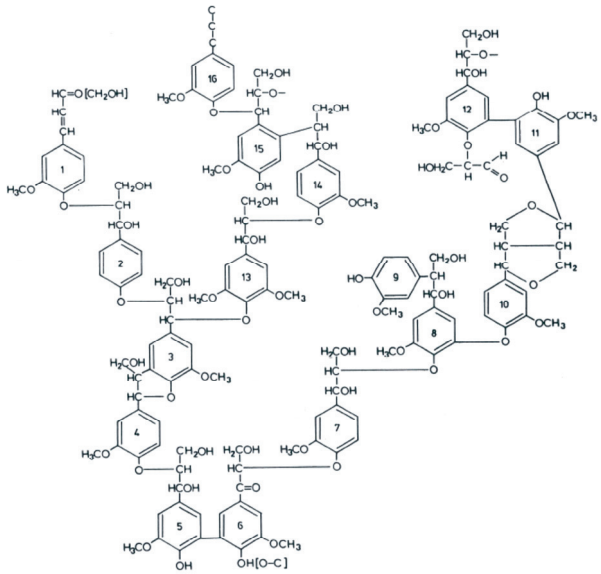

Fig. 1.10 A structural segment of softwood lignin proposed by Adler in 1977 (Sjöström **1993**).

1.4 Hemicelluloses

The main function of the hemicelluloses is to crosslink the cellulose fibrils with the lignin matrix. The hemicelluloses and celluloses together are often referred to as *holocellulose*. In contrast to cellulose, the hemicelluloses are heteropolysacharides, with their monomeric components consisting of anhydrohexoses (D-glucose, D-mannose and D-galactose), anhydropentoses (D-xylose and L-arabinose) and Anhydrouronic acids (D-glucuronic acid, D-galacturonic acid). Most hemicelluloses have a DP of only 200. Some wood hemicelluloses are extensively branched and are readily soluble in water. An example is *Gum Arabic* which is exuded as a viscous fluid at sites of injury of tropical trees. Hemicelluloses usually account for 20 to 30% w/w of the dry weight of wood. The composition and structure of the hemicelluloses in softwood differ in a characteristic way from those in hardwoods (Sjöström **1993**).

In softwood, the principal hemicelluloses are *galactoglucomannans* (about 20%). Their backbone consists of a linear chain built up by β(1→4) linked D-glucopyranose and β(1→4) linked D-mannopyranose units. The α-D-galactopyranose units are linked as a single unit side chain to the framework by (1→6) bonds (Fig. 1.11). The galactoglucomannans can be roughly divided in two groups, one with low galactose content (galactose:glucose:mannose 0.1:1:4) and one with a higher amount of galactose (1:1:4).

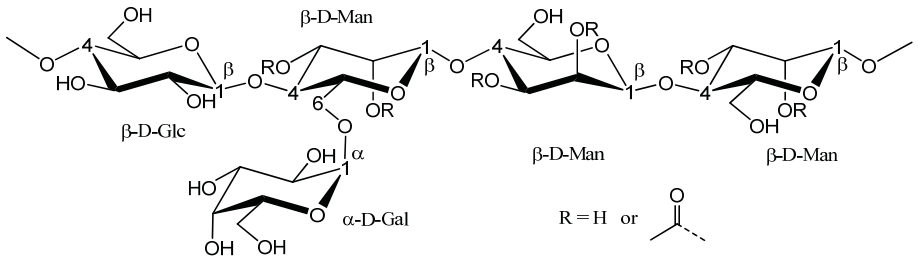

Fig. 1.11 Principal structure of galactoglucomannans. Sugar units: β-D-glucopyranose (β-D-Glc); β-D-mannopyranose (β-D-Man); α-D-galactopyranose (α-D-Gal) (Sjöström **1993**).

In addition to galactoglucomannans, softwoods also contain *arabinoglucuronoxylan* (about 5-10%). It is composed of a linear framework of β(1→4) linked D-xylopyranose units. Partially, they are substituted at the C2 by 4-O-methyl-α-D-glucuronic acid groups. In addition, the framework contains also some α-L-arabinofuranose units (Fig. 1.12).

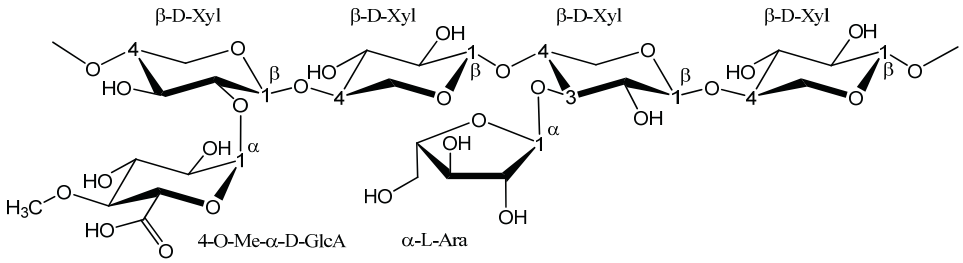

Fig. 1.12 Principal structure of arabinoglucuronoxylan. Sugar units: β-D-xylopyranose (β-D-Xyl); 4-O-methyl-α-D-glucopyranosyluronic acid (α-D-GlcA); α-L-Arabinofuranose (α-L-Ara) (Sjöström **1993**).

Other polysaccharides in softwoods are arabinogalactan (predominantly in larches), starch (which is composed of amylose and amylopectin) or pectic substances.

In hardwood, the major hemicellulose component is an O-acetyl-4-O-methylglucurono-β-D-xylan, sometimes called *glucuronoxlyan*. Depending on the hardwood species, the xlyan content varies within 15-30% w/w of the dry wood. The backbone consists of β(1→4) linked D-xylopyranose units. About seven of ten xylose units contain an O-acetyl group at the C2 or C3. In addition, per ten xylose units there is on average one (1→2) linked 4-O-methyl-α-D-glucuronic acid residue (Fig. 1.13).

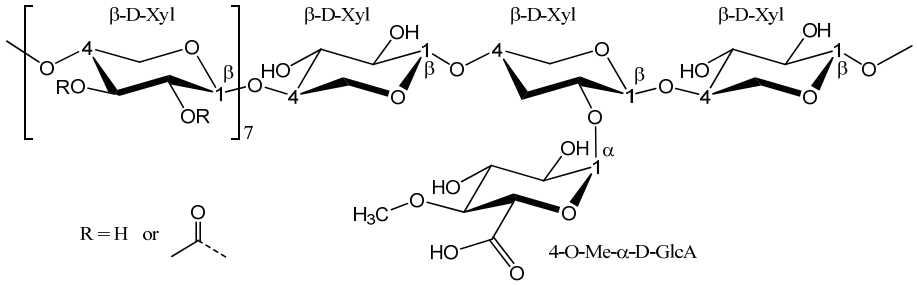

Fig. 1.13 Principal structure of glucuronoxlyan. Sugar units: β-D-xylopyranose (β-D-Xyl); 4-O-methyl-α-D-glucopyranosyluronic acid (α-D-GlcA) (Sjöström **1993**).

In addition to xlyan, hardwoods also contain *glucomannan* (about 2-5%). It is composed of a linear framework of β(1→4) linked D-glycopyranose and D-mannopyranose units. The ratio between glucose and mannose varies between 1:1 and 1:2. The structure of glucomannan is the same as for galactoglucomannan in Figure 1.11 when omitting the galactopyranose residue. As for the softwoods, there are minor amounts of other polysaccharides present in hardwoods, partly of the same type (Sjöström **1993**).

1.5 Hornification

The strength properties of paper made from dried and rewetted low-yield pulp (kraft pulp) are inferior to those of paper made from the same fibers that were never dried. More precisely, repeated drying of pulp results in a progressive loss of its swelling ability and in a decrease of its burst, fold and tensile strength. This loss in strength is typical for recycled fibers, originating from a structural change in the cell wall and is called *hornification*. High-yield pulp is hardly affected by this process (Jayme **1944**; Lindström and Carlsson **1982;** Scallan and Tigerström **1992**).

The structural change in the cell wall was attributed to irreversible agglomeration of microfibrils of neighboring lamellae (tangentially oriented planes of microfibrils) between and within the different layers of the cell wall. During swelling of pulp (Fig. 1.14) adjacent microfibrils of neighboring lamellae are debonded by suitable agents. During drying, additional hydrogen bonds are formed irreversibly between the microfibrils of neighboring lamellae and the pores in the cell wall structure close (Scallan **1974**; Lindström and Carlsson **1982**).

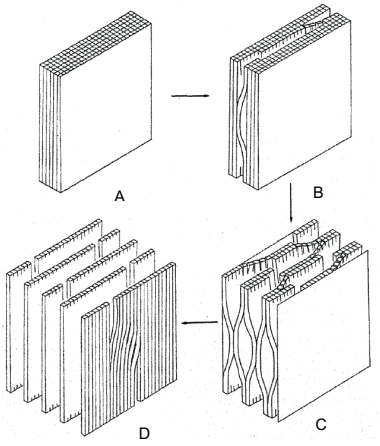

Fig. 1.14 Cell-wall model for the swelling process: fiber wall dried from water *(A)*, initiation of swelling by suitable swelling agents *(B)*, further breaking of hydrogen bonds by water in an intermediate state of swelling *(C)* and complete delamination (swelling) of the lamellae *(D)* (Scallan **1974**).

To estimate the degree of hornification, the water retention value (WRV) can be measured, which is the amount of water retained by a pad of wet pulp after centrifugation for ten minutes at 2300 rpm. The WRV of Kraft pulp decreases significantly upon repeated drying and redispersion of the fibers in water (Jayme **1944**).

The introduction of carboxylate groups in their deprotonated form onto cellulose fibers led to an increase in the WRV value for dried and redispersed fibers. For a sufficiently large amount of carboxylate groups (corresponding to a DS of approximately 0.05), the WRV remained constant, regardless of the pulp being dried or not. In the protonated form, there was no effect of the carboxyl groups on the WRV, suggesting severe hornification of the pulp upon drying (Lindström and Carlsson **1982**).

There were two mechanisms suggested by the authors to understand these effects. The first explanation involved the ability of the carboxyl groups in their protonated form to establish hydrogen bonding. In their deprotonated form, however, the ability of the carboxylate groups to form hydrogen bonds was regarded to be lower. This in turn might then create interruptions in the sequence of consecutive hydrogen bonds between microfibrils of neighboring lamellae. A second suggestion was the formation of ester bonds between the carboxyl groups and hydroxyl groups of adjacent microfibrils under acidic conditions, as for instance lactone formation (Lindström and Carlsson **1982**).

However, the mechanism of hornification as well as the effect of the carboxylate and carboxyl groups on the hornification process does not seem completely convincing. First, the carboxylate group can also interact with the proton of an alcoholic group (in a type of hydrogen bonding through the delocalized negative charge). And second, the formation of a lactone (or an ester in general) requires energy and is therefore not expected to occur during drying at room temperature.

Nevertheless, it was shown that carboxymethylation of cellulose is a suitable method to prevent hornification of the fibers during drying.

1.6 Objectives

A first aim of this work was to isolate NFC from a never-dried wood pulp (refined and bleached beech pulp, RBP) and chemically modify it in a way that allows drying the product to a powder. A method to prevent hornification during the drying process was elaborated, developed from earlier findings about carboxymethylation of pulp from literature. A second step was compounding NFC in powder form with biopolymers to estimate its reinforcing effect in a nanocomposite. The final goal was the comparison of the results of mechanical tests obtained from dried NFC powder with those obtained from never-dried NFC to evaluate the effectiveness of the method to prevent hornification of NFC during drying.

2 Experimental Procedures

2.1 Materials

Refined and bleached beech pulp (RBP) was provided by J. Rettenmaier & Söhne GmbH, Rosenberg, Germany (Arbocel B1011, M_{AGU} = 162.14 g/mol, 10.0% w/w aqueous suspension). Carboxymethylation of the pulp was performed with mono-chloroacetic from Merck (sodium salt, purity ≥ 98%, M = 116.48 g/mol). A commercial poly(vinyl acetate) (PVAc) latex, VN 1693 (Collano AG, Switzerland) with a solids content of 49.5 ± 0.1% was used as a matrix for the preparation of nanocomposites with NFC. The latex is an aqueous suspension of PVAc particles stabilized by PVOH and it does not contain cross-linking agents. Hydroxypropyl cellulose (HPC) with a molecular substitution (MS) of 3.4 – 4.4 and a weight-average molecular weight (Mw) of 100'000 was purchased from Sigma-Aldrich Chemie GmbH (Steinheim, Germany).

2.2 Mechanical Isolation of NFC

Isolation of NFC from the RBP raw material was performed in a three step procedure. First, the pulp was dispersed and swollen in water. Second, it was mechanically pre-treated, using an Ultra-Turrax system (Megatron MT 3'000, Kinematica AG, Luzern, Switzerland) (Fig. 2.1 *left*). Finally, the fibrils were mechanically isolated from the pulp in a high-shear laboratory homogenizer (Microfluidizer type M-110Y, Microfluidics Corporation, USA) (Fig. 2.1 *rigtht*).

The swelling of the pulp and the mechanical pre-treatment using the Ultra-Turrax system was crucial for a continuous and smooth operation of the laboratory homogenizer. Large fiber fragments or impurities were found to clog the interaction chambers. Within these chambers the pre-treated aqueous fiber suspension is forced through thin capillaries (with diameters between 75 and 400 μm, depending on the chamber type) of specific geometries under large pressure (typically around 100MPa). Due to the high pressure, there occur high shear-forces at the edges of the capillaries that lead to a disruption of the fibers into fibril aggregates.

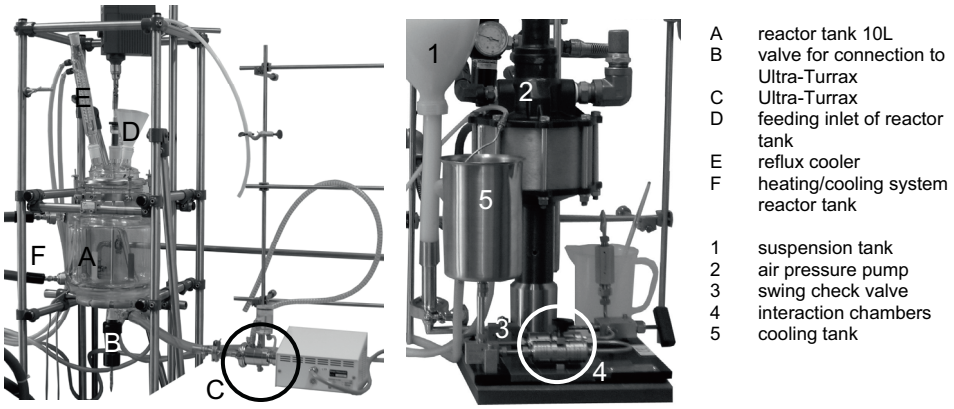

Fig. 2.1 Photographs of the inline-dispersing system containing a 10L glass reactor and an Ultra-Turrax *(left)* and of the laboratory homogenizer with the two interaction chambers *(right)*.

The mechanically treated fibril suspension is then cooled and fed back to the suspension tank. By measuring the flux (throughput of suspension in weight per time) the number of passes can be determined. The final product is yielded as a suspension with a concentration of approximately 1 to 2 % w/w.

Optionally, the glass reactor (Fig. 2.1 left) was used to perform a carboxymethylation reaction onto the RBP under reflux at controlled temperature (60°C). The chemical modification of the fibers can be done after or before the isolation of the fibrils using the laboratory homogenizer.

2.3 Tests and Analysis

Several methods were used to confirm the successful chemical modification and isolation of NFC. Fourier-Transform Infrared Spectroscopy (FT-IR) and Solid-State Cross Polarization Magic Angle Spinning Nuclear Magnetic Resonance Spectroscopy (^{13}C CP-MAS NMR) were used to determine the chemical structure of the products from the carboxymethylation reaction. The degree of substitution (DS) was measured by Conductometric Titration (CT). The crystallinity and the thermal stability of the final NFC products were measured by X-Ray Diffraction (XRD) and Thermogravimetric Analysis (TGA), respectively. The morphology of the isolated NFC samples was characterized by Scanning Electron Microscopy (SEM). Mechanical properties (storage modulus, tensile strength, modulus of elasticity [MOE] and tensile strain at break) were measured by Dynamic Mechanical Analysis (DMA) and tensile testing, respectively.

3 Summary of appended papers

Paper I: Preparation and characterization of water-redispersible nanofibrillated cellulose in powder form

The first paper aimed at the development of a suitable method for the preparation of NFC in powder form. It was earlier reported that carboxymethylation can reduce hornification in drying and rewetting cycles of pulp fibers. Two routes were investigated for the preparation of carboxymethylated NFC powder by interchanging the sequence of the chemical modification and the mechanical isolation step. A drying method was developed, including solvent exchange to alcohol and repeated stirring during drying in an oven. Depending on the DS, the final powders showed good redispersibility in water and formed stable suspensions for several hours. Generally, both routes proved to be feasible for the preparation of redispersible NFC in powder form. However, the clearly lower number of chamber clogging and the better quality of the isolated NFC (the size and the homogeneity of distribution of the fibril diameter) showed that it is more effective to first carboxymethylate the RBP and then apply the mechanical isolation in a second step, rather than the interchanged sequence.

Paper II: DMA analysis and wood bonding of PVAc latex reinforced with cellulose nanofibrils

The aim of the second paper was to prepare nanocomposites with carboxymethylated NFC and commercial PVAc latex and to investigate the mechanical reinforcing effect of the chemically modified NFC. The composites were prepared by mixing the components in water and degassing the suspensions under vacuum, before casting the films onto silicon molds. Rectangular shaped samples were cut off the films, dried and finally measured by DMA in tensile mode. The results showed a strong increase of the storage modulus in the rubbery plateau with increasing concentration of NFC for all composites prepared, compared to the neat PVAc. The same trend was observed for the storage modulus in the glassy state. In addition, the presence of the NFC led to a gradual disappearance of the tan δ peak in the PVOH glass transition around 80°C, suggesting strong interaction between the NFC and the PVOH. Again, DMA experiments showed that the combination of chemical modification, followed by mechanical disintegration leads to the strongest reinforcing effects.

In addition, three PVAc formulations (neat PVAc and PVAc containing carboxymethylated RBP of 1 and 3% w/w, respectively) were also tested as adhesives, by

preparing bonded panels of beech wood. The assemblies were tested for Durability class D1 (conditioning 7 days in standard atmosphere), Durability class D3 (as D1 plus 4 days in water at 20°C) and WATT ’91 (as D1 plus 60min at 80°C). The adhesives all passed durability class D1 but failed test D3 (which was surprising, since the PVAc adhesive was classified as suitable for class D3 by the provider). However, the addition of the carboxymethylated fibers led to a significant increase in heat resistance of the boards, as deduced from the WATT ’91 test.

Paper III: Reinforcing effect of carboxymethylated nanofibrillated cellulose powder on hydroxypropyl cellulose

In the third paper, the reinforcing potential of the carboxymethylated NFC powders was compared to the reinforcing potential of their never-dried analogues. Nanocomposites were prepared from carboxymethylated NFC and hydroxypropyl cellulose (HPC) by solution casting. Reference materials containing only mechanically treated NFC, untreated RBP or no fibers, respectively, were also prepared and compared to the nanocomposites.

The mechanical properties of the composites were measured by DMA and tensile testing. The results showed that the mechanical properties (storage modulus, tensile strength, MOE and tensile strain at break) of carboxymethylated NFC were the same, regardless whether the NFC was dried and redispersed or not before compounding. In contrast, the composites containing NFC without carboxylate groups showed clearly inferior values for storage modulus, tensile strength and MOE when the NFC was dried and redispersed). In addition, SEM images showed a homogeneous, layered morphology for freeze-fractured composites containing carboxymethylated NFC that was dried to a powder. The freeze-fractured samples prepared with chemically unmodified NFC powder, however showed large agglomerations and voids, indicating severe agglomeration of the fibrils.

4 Conclusions

This study has shown that carboxymethylation of RBP prior to mechanical disintegration is a suitable method to prepare NFC in powder form without the disadvantageous effects of hornification. The powders can be redispersed in water and form stable suspension for several hours. The proposed method allows shipping and storage of NFC in dry form without the loss of its mechanical and morphological properties, therefore reducing costs due to lower weight and volume. In addition, the easier handling of the NFC powder compared to the conventional aqueous suspensions (e.g. no need for solvent exchange to alcohol for further chemical modification, easier and more accurate determination of the weight of the dry material) might be another important advantage.

It can be concluded that in hydrophilic, thermoplastic polymer matrices like PVAc or HPC the NFC powder can lead to an increase in thermal stability above the glass temperature of the polymer, due to a percolating network effect. This increase in thermal stability might be limited above the degradation temperature of 200°C of the NFC powder. Also, there has been evidence that the NFC powders can slightly increase the storage moduli in the glassy state of these polymers.

5 Outlook

Future studies will focus on the preparation of nanocomposites containing other biopolymers and NFC powders. One important aspect will be the incorporation of NFC in hydrophobic polymer matrices. For this purpose, the NFC powders must be further chemically modified to match the different surface energies of the matrices (secondary forces) or to be irreversibly attached to the matrix by covalent bonds (primary forces).

Another aspect will be to evaluate the feasibility of preparing nanocomposites from NFC powders and biopolymers by extrusion. This industrial process is highly important for the up scaling of possible products.

6 Acknowledgements

This work was carried out at the Wood Laboratory of the Department of Civil and Mechanical Engineering at the Swiss Federal Laboratories for Materials Science and Technology (EMPA) in Dübendorf, Switzerland, in collaboration with the Division of Manufacturing and Design of Wood and Bionanocomposites at Luleå University of Technology (LTU) in Luleå, Sweden.

I would like to express my gratitude to my supervisors, Prof. Kristiina Oksman Niska (LTU) and Dr. Tanja Zimmermann (EMPA), for their guidance and careful revision of my work.

My thanks go also to Nico Bordeanu and Philippe Tingaut for their valuable help in the lab and for all the interesting, scientific discussions.

For entertaining working days and coffee breaks I owe my thanks to my PhD colleagues “Jessie” Zheng Zhang, “Thao” Thuthao Ho, “Chrille” Christian Lehringer und Robert Jockwer.

For his helpful support in Sweden, my thanks go to Göran Grubbström.

The financial support State Secretariat for Education and Research (SER) is greatfully acknowledged.

7 References

Azizi Samir MAS, Alloin F, Paillet M, Dufresne A **2004** Tangling effect in fibrillated cellulose reinforced nanocomposites 37, 4313-4316

Besseuille L, Bulone V **2008** A survey of cellulose biosynthesis in higher plants. Plant Biotechn 25, 315-322

Boldizar A, Klason C, Kubat J, Naslund P, Saha P **1987** Prehydrolyzed cellulose as reinforcing filler for thermoplastics. Int J of Polym Mat 11, 229-262

Diotallevi F, Mulder B **2007** The cellulose synthase complex: a polymerization driven supramolecular motor. Biophys J 92, 2666-2673

Delmer DP **1987** Cellulose biosynthesis. Ann Rev Plant Physiol 38, 259-290

Dufresne A, Vignon MR **1998** Improvement of starch film performances using cellulose microfibrils. Macromolecules 31, 2693-2696

Ek M, Gellerstedt G, Henriksson G **2009** Pulp and paper chemistry and technology, volume 2: pulping chemistry and technology. Walter de Gruyter GmbH & Co. Berlin

Favier V, Chanzy H, Cavaillé JY **1995** Polymer nanocomposites reinforced by cellulose whiskers. Macromolecules 28, 6365-6367

Herrick FW, Casebier RL, Hamilton JK, Sandberg KR **1983** Microfibrillated cellulose: morphology and accessibility. J Appl Polym Sci: Appl Polym Symp 37, 797-813

Hubbe MA, Rojas OJ, Lucia LA, Sain M **2008** Cellulosic nanocomposites: a review. Biores 3, 929-980

Jayme G **1944** Mikro-Quellungsmessungen an Zellstoffen. Wochenbl f Papierfabr 42, 187-194

Klemm D, Heublein B, Fink HP, Bohn A **2005** Cellulose: fascinating biopolymer and sustainable raw material. Angew Chem Int Ed 44, 3358-3393

Laivins GV, Scallan AM **1993** The mechanism of hornification of wood pulps. Proc 10th fund res symp. Oxford, pp 1235–1260

Lindström T, Carlsson G **1982** The effect of carboxyl groups and their ionic form during drying on the hornification of cellulose fibers. Svensk Papperstidning 85, R146-R151

Oksman K, Mathew AP, Bondeson D, Kvien I **2006** Manufacturing process of cellulose whiskers/polylactic acid nanocomposites. Comp Sci and Techn 66, 2776-2784

O'Sullivan AC **1997** Cellulose: the structure slowly unravels. Cellulose 4, 173-207

Petersson L, Kvien I, Oksman K **2007** Structure and thermal properties of poly(lactic acid)/cellulose whiskers nanocomposite materials. Comp Sci and Techn 67, 2535-2544

Scallan AM **1974** The structure of the cell wall in wood – A consequence of anisotropic inter-microfibrillar bonding? Wood Sci 6, 266-271

Scallan AM, Tigerström AC **1992** Swelling and elasticity of the cell walls of pulp fibres. J Pulp Paper Sci 18, J188-J193

Siró I, Plackett D **2010** Microfibrillated cellulose and new nanocomposite materials: a review. Cellulose 17, 459-494

Sjöström E **1993** Wood chemistry: fundamentals and applications (second edition). Academic press, inc. San Diego, California

Turbak AF, Snyder FW, Sandberg KR **1983** Microfibrillated cellulose, a new cellulose product: properties, uses, and commercial potential. J Appl Polym Sci: Appl Polym Symp 37, 815-827

Young RA **1994** Comparison of the properties of chemical cellulose pulp. Cellulose 1 107-130

Zadorecki P, Michell AJ **1989** Future prospects for wood cellulose as reinforcement in organic polymer composites. Polym Comp 10, 69-77

Zimmermann T, Pöhler E, Geiger T **2004** Cellulose fibrils for polymer reinforcement. Adv Eng Mat 6, 754-761

Paper I

Cellulose (2010) 17:19–30
DOI 10.1007/s10570-009-9372-3

Preparation and characterization of water-redispersible nanofibrillated cellulose in powder form

Ch. Eyholzer · N. Bordeanu · F. Lopez-Suevos · D. Rentsch · T. Zimmermann · K. Oksman

Received: 16 July 2009 / Accepted: 5 October 2009 / Published online: 20 November 2009

Abstract Water-redispersible, nanofibrillated cellulose (NFC) in powder form was prepared from refined, bleached beech pulp (RBP) by carboxymethylation (c) and mechanical disintegration (m). Two routes were examined by altering the sequence of the chemical and mechanical treatment, leading to four different products: RBP-m and RBP-mc (route 1), and RBP-c and RBP-cm (route 2). The occurrence of the carboxymethylation reaction was confirmed by FT-IR spectrometry and ^{13}C solid state NMR (^{13}C CP-MAS) spectroscopy with the appearance of characteristic signals for the carboxylate group at 1,595 cm^{-1} and 180 ppm, respectively. The chemical modification reduced the crystallinity of the products, especially for those of route 2, as shown by XRD experiments. Also, TGA showed a decrease in the thermal stability of the carboxymethylated products. However, sedimentation tests revealed that carboxymethylation was critical to obtain water-redispersible powders: the products of route 2 were easier to redisperse in water and their aqueous suspensions were more stable and transparent than those from route 1. SEM images of freeze-dried suspensions from redispersed RBP powders confirmed that carboxymethylation prevented irreversible agglomeration of cellulose fibrils during drying. These results suggest that carboxymethylated and mechanically disintegrated RBP in dry form is a very attractive alternative to conventional NFC aqueous suspensions as starting material for derivatization and compounding with (bio)polymers.

Keywords Cellulose · Carboxymethylation · Mechanical disintegration · Nanofibrils · Hornification · Water-redispersible

Ch. Eyholzer (✉) · N. Bordeanu · F. Lopez-Suevos · D. Rentsch · T. Zimmermann
Swiss Federal Laboratories for Materials Testing and Research (EMPA), Dübendorf, Switzerland
e-mail: christian.eyholzer@empa.ch

Ch. Eyholzer · K. Oksman
Division of Manufacturing and Design of Wood and Bionanocomposites, Luleå University of Technology (LTU), Luleå, Sweden

Introduction

Nanofibrillated cellulose (NFC) has attracted great interest for the preparation of nanocomposites with polymer matrices due to its interesting properties, such as high strength and stiffness (Zadorecki and Michell 1989; Yano and Nakahara 2004; Hubbe et al. 2008), transparency (Yano et al. 2005) or biodegradability (Couderc et al. 2009). The isolation of NFC from wood pulp has been achieved by applying mechanical treatment, using a high-pressure homogenizer (Turbak et al. 1983; Herrick et al. 1983; Wågberg et al. 1987; Pääkkö et al. 2007) or grinding with previous chemical treatment (Abe et al. 2007; Saito et al. 2006). However, the hydrophilic nature of

cellulose causes two major issues, namely, irreversible agglomeration during drying and agglomeration of NFC in non-polar matrices during compounding.

Irreversible agglomeration of cellulose during drying is called hornification (Young 1994; Hult et al. 2001) and is explained by the formation of additional hydrogen bonds between amorphous parts of the cellulose fibrils during drying. The formation of these bonds correlates with the amount of water removed, and does not depend directly on temperature. As in the crystalline parts of cellulose, water cannot break the formed hydrogen bonds during rewetting of hornificated cellulose (Scallan and Tigerström 1992; Laivins and Scallan 1993). To prevent hornification, isolation of NFC is preferentially done by mechanical disintegration of never-dried pulp in an aqueous suspension. So far, to the best of the authors' knowledge, there is only one commercially available NFC product of high quality (Celish, Daicel Chemical Industries, Osaka, Japan), which is delivered as a 10–35% (w/w) aqueous suspension. The ramifications of producing NFC in aqueous suspensions are high shipping costs, large storage facilities and propensity towards bacterial decomposition. Consequently, the preparation of a nanofibrillated cellulose powder, which can be easily dispersed in water avoiding hornification, would be of great industrial interest from both economical and ecological points of view. Also, the general interest in preparing NFC powder avoiding hornification has been evidenced in several patents (Herrick 1984; Bahia 1995; Dinand et al. 1996; Excoffier et al. 1999; Cantiani et al. 2001; Cash et al. 2003; Bordeanu et al. 2008). Basically, the main strategy is prevention of increased hydrogen bond formation between cellulose fibrils by introducing steric and electrostatic groups.These groups increase the accessibility and affinity of water towards the fibrils.

The second issue is agglomeration of NFC in hydrophobic polymers during compounding. Again it is the large number of hydrogen bonds that can be formed between the cellulose fibrils that prevent a homogeneous distribution of NFC within a non-polar polymer matrix. Therefore, the aspect ratio of these NFC agglomerates is drastically reduced, causing a strong decrease in their reinforcing potential (Boldizar et al. 1987; Chakraborty et al. 2006). In order to improve compatibility at the fiber-matrix interface, chemical modification of cellulose hydroxyl groups is a viable and widely used approach. Various methods to modify the surface of NFC were reported, such as silylation (Goussé et al. 2004; Andresen et al. 2006), TEMPO oxidation (Saito et al. 2006; Araki et al. 2001; Lasseuguette 2008), acetylation (Sassi and Chanzy 1995) or reactions with anhydrides (Stenstad et al. 2008).

Partial carboxymethylation of the NFC hydroxyl groups can overcome hornification during drying, provided that the carboxylic groups are present in their sodium form (Lindström and Carlsson 1982; Laivins and Scallan 1993). Also, this effect depends on the degree of substitution (DS) which is defined by the ratio of reacted carboxyl groups per anhydroglucose units (AGU). The DS of commercially available carboxymethyl cellulose (CMC) is usually between 0.5 and 1.0 but mainly around 0.9. Such highly water-soluble CMC is well-known as a thickening agent in food, as an additive in pharmaceutics, cosmetics and detergents, but also as a component of membranes or drilling mud for water retention. Below a DS of 0.3–0.4, CMC is insoluble in water, however, such low-DS CMC show higher water absorbance and swelling in water than the original cellulose, even if the DS is only 0.025 (Walecka 1956; Reid and Daul 1947). In addition to the prevention of hornification, carboxymethylation could possibly also prevent agglomeration of the NFC during compounding with polymers. However, further chemical modification to enhance the chemical affinity of the NFC to different non-polar polymer matrices might be necessary.

In the present work, two routes for the preparation of dry, water-redispersible NFC are compared by altering the sequence of the chemical and mechanical treatment of a commercial, refined beech pulp (RBP). The resulting modified and unmodified RBP powders were analyzed by FT-IR, ^{13}C solid state NMR (^{13}C CP-MAS), XRD and TGA in order to learn more about their chemical structure and thermal stability. Also, after dispersing the RBP powders in water, sedimentation studies were conducted to evaluate the stability of the different suspensions. Finally, the redispersed RBP suspensions were freeze-dried and their morphologies were analyzed by the SEM.

Materials and methods

Refined, bleached beech pulp (RBP) was provided by J. Rettenmaier & Söhne GmbH, Rosenberg, Germany

(Arbocel B1011, 10.0% w/w aqueous suspension, M_{AGU} (anhydroglucose unit) = 162 g/mol). Chloroacetic acid (sodium salt, purity ≥ 98%, M = 116.48 g/mol) and sodium hydroxide (NaOH, purity ≥ 98%, M = 40.0 g/mol) were purchased from Merck and Fluka, respectively.

Mechanical disintegration

Preparation of RBP-m (route 1) was performed in a 10 L glass reactor, equipped with an inline Ultra-Turrax system (Megatron MT 3,000, Kinematica AG, Luzern, Switzerland), and in a high-shear homogenizer (Microfluidizer type M-110Y, Microfluidics Corporation, USA). 2.0 kg of the 10% w/w aqueous RBP were diluted to 2.0% w/w with 8.0 kg of deionised water and allowed to swell for one week at 20 °C, followed by 2 h of homogenization using the Ultra-Turrax system (20,000 rpm). The suspension was diluted with deionised water to 1.75% w/w and pumped through a $H230Z_{400\ \mu m}$ and a $H30Z_{200\ \mu m}$ chamber for 6 passes, followed by another 4 passes through a $H230Z_{400\ \mu m}$ and a $F20Y_{75\ \mu m}$ chamber. The processing pressure inside the F20Y chamber was calculated to approximately 125 MPa. The resulting RBP-m suspension was then concentrated to a dry material content of 10.0% in a centrifuge (5,000 rpm, 15 °C, 45 min).

For the preparation of RBP-cm (route 2), 8.75 g of RBP-c (solid, preparation described below) were used as starting material. The RBP-c powder was dispersed in 500 ml of deionised water to a final concentration of 1.75% w/w and homogenized with a blender (T 25 basic, IKA-Werke, Staufen, Germany). In general, the mechanical treatment of the resulting suspension was performed as previously described for route 1. However, the disintegration treatment was stopped after only 2–3 passes through the $H230Z_{400\ \mu m}$ and $F20Y_{75\ \mu m}$ chambers since the resulting gel became too viscous for further processing.

Chemical modification

Preparation of RBP-mc (route 1) was performed in a 10 L glass reactor, equipped with the Ultra-Turrax system and a mechanical stirrer. 700 g of the 10% w/w aqueous RBP-m suspension (0.432 mol AGU) was transferred into the reactor. 6.2 L of a 5/3 v/v isopropanol/ethanol mixture was added to obtain a final cellulose concentration of 1.27% w/w. The suspension was homogenized, using the Ultra-Turrax system (10,000 rpm; 20 °C). After 15 min, 303 g of a 5.0% w/w NaOH aqueous solution (0.4 mol) was added dropwise to the RBP-m for 30 min to activate the cellulose. Then, 25.1 g of chloroacetic acid (sodium salt; 0.216 mol) was added to the activated RBP. The mixture was heated to 60 °C under stirring, without using the Ultra-Turrax system. The reaction was stopped after 2 h by cooling it to room temperature and the pH of the suspension was adjusted to neutrality with acetic acid.

Preparation of RBP-c (route 2) was performed with 700 g of the 10% w/w RBP aqueous suspension (0.432 mol AGU) as starting material. In this case, 198 g of a 5.0% w/w aqueous NaOH solution (0.25 mol) and 14.85 g of chloroacetic acid (sodium salt; 0.127 mol) was used.

Purification of RBP-mc and RBP-c was done by washing them several times with different solutions (described below) and centrifugation (5,000 rpm, 15 °C, 45 min). First, the glycolic acid (by-product) was removed with a 1/1 v/v mixture of 0.05 M aqueous acetic acid and 5/3 v/v isopropanol/ethanol. Second, the carboxyl groups of the modified cellulose were deprotonated with a 1/1 v/v mixture of 0.05 M aqueous NaOH and 5/3 v/v isopropanol/ethanol. Finally, the remaining salts were washed off with a 1/1 v/v mixture of deionised water and 5/3 v/v isopropanol/ethanol. It was ensured that the pH of the last supernatant did not drop below 8.0.

Drying of cellulose suspensions

To obtain cellulose powders from aqueous suspensions of the various samples, a two steps procedure was applied. First, the solvent of the aqueous suspensions was exchanged from deionised water to a 5:3 v/v isopropanol/ethanol mixture in several washing and centrifugation steps (5,000 rpm, 15 °C, 45 min). Then, the suspensions were stirred several times with a glass bar during drying in an oven at 60 °C, until a fine powder of constant weight was obtained.

Determination of the degree of substitution (DS)

Conductometric titration (CT) was used to calculate the DS of carboxymethylated RBP following the protocol of Eyler (Eyler et al. 1947) with slight modifications. 0.3 g of dried, carboxymethylated cellulose fibrils were redispersed in 60.0 g of deionised water using a blender. Then, 5.0 ml of a 0.1 M aqueous NaOH solution was added to the suspension and stirred with a magnetic bar. The conductivity of the suspension was measured upon titration with 10.0 ml of a 0.1 M aqueous hydrochloric acid (HCl) solution, using a Metrohm conductometer (model 1.712.0010, Metrohm AG, Herisau, Switzerland), equipped with a platinum electrode (model 6.0309.100). The measurements were repeated three times for each sample. The experimental DS values for RBP-mc (0.087 ± 0.002), RBP-c (0.130 ± 0.001) and RBP-cm (0.138 ± 0.002) were significantly lower than those expected stoichiometrically (0.3 and 0.5, respectively). This difference can be attributed to the partial deactivation of monochloroacetic acid with water during the reaction and the loss of some higher substituted, water-soluble NFC during purification.

Fourier transform-infrared spectroscopy (FT-IR)

Powder samples were measured after drying at 60 °C. The spectra were recorded using a Digilab BioRad FTS 6000 Spectrometer (Philadelphia, USA) in single reflection diamond ATR (Attenuated Total Reflectance) mode (P/N 10,500 series, golden gate). The number of scans was 32 and the resolution was 4 cm^{-1}.

Solid-state ^{13}C CP-MAS NMR spectroscopy (Cross Polarization Magic Angle Spinning Nuclear Magnetic Resonance)

The ^{13}C CP-MAS NMR spectra of the RBP samples were measured at 100.61 MHz on a Bruker AVANCE -400 MHz NMR Spectrometer (Bruker BioSpin AG, Fällanden, Switzerland) using a 7 mm broadband CP-MAS probe. The following parameters were used: MAS rates of 3,000 Hz, CP-MAS contact times of 3 ms, 8 s relaxation delays, number of accumulated free induction decays (FID) > 20,000 (for a reasonable signal to noise ratio of the carbonyl resonances, 2,134 for the untreated RBP) applying 38 kHz TPPM decoupling of ^{1}H during acquisition. The FIDs were multiplied by an exponential window function of 50 Hz before Fourier Transformation.

X-Ray diffraction (XRD)

For each RBP, three pellets were prepared by applying 3 t of weight to 750 mg of powder for 2 min. The pellets were measured in reflection mode, using an X'Pert Pro diffractometer from Panalytical (Almelo, Netherlands) with Cu K_α radiation ($\lambda = 1.5418$ Å) in combination with a linear detector system (X'Celerator).

Thermogravimetric analysis (TGA)

Degradation behavior of the treated and untreated RBP was analyzed using a NETZSCH TG 209 F1 (Netzsch Group, Selb, Germany) in dry gas nitrogen atmosphere. The heating rate was 20 °C/min.

Scanning electron microscopy (SEM)

The prepared cellulose powders of both routes were redispersed in water to a final concentration of 0.1% w/w and homogenized with a blender. Then, a sample holder on which a fresh mica plate had been fixed with liquid carbon cement was cooled down in liquid nitrogen. Immediately after removing the sample holder plate, droplets of the 0.1% w/w suspensions of the treated and untreated RBP in water were placed onto the surface with a syringe. The frozen sample was then kept under vacuum (below 1×10^{-1} mbar) until the ice was sublimated. The freeze-dried RBP samples were then sputtered with a 4 nm platinum coating. Images were recorded in a JEOL JSM-6300F (Jeol Ltd., Tokyo, Japan) equipped with a cold-cathode field emission gun. The following parameters were used: acceleration voltage of 5.0 kV, probe current of 6×10^{-11} A, working distance of 48 mm. Of each suspension, three droplets were analyzed. All images were recorded in the center of the droplets.

Results and discussion

Two processing routes (Fig. 1) were proposed to prepare nanofibrillated cellulose powder, capable of

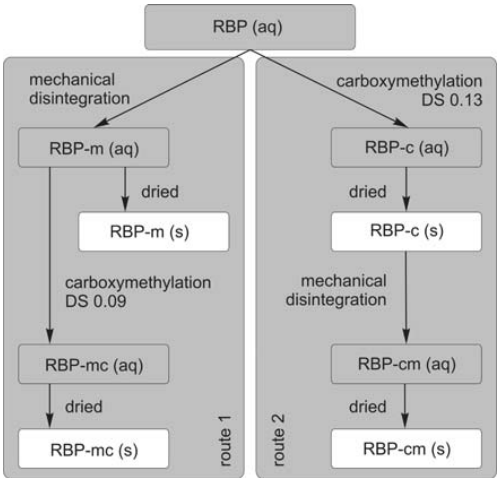

Fig. 1 Schematic overview on the sample preparation routes. In route 1 (*left block*), the untreated RBP is mechanically disintegrated (RBP-m), followed by carboxymethylation (RBP-mc). In route 2 (*right block*), the treatments are interchanged. The untreated RBP was first carboxymethylated (RBP-c), then dried to a powder, redispersed in water and finally mechanically disintegrated (RBP-cm). Aqueous suspensions (*grey*) are intermediate products

forming a stable suspension after redispersion in water. Mechanical disintegration of the pulp was done either before (route 1) or after (route 2) carboxymethylation (Fig. 2). Good redispersibility of the final RBP powder in water depended on the drying procedure and the DS of the CMC. Drying CMC from a 5:3 v/v isopropanol/ethanol mixture at 60 °C under occasional stirring with a glass bar led to a highly porous and fluffy powder with a significantly higher volume compared to those dried from aqueous suspensions or without stirring. This can directly account for the enhanced redispersibility of the powders in water, being able to more easily penetrate the more open structure of the cellulose. The use of a blender for several seconds of course accelerates the re-wetting of the cellulose. No further treatment (e.g.

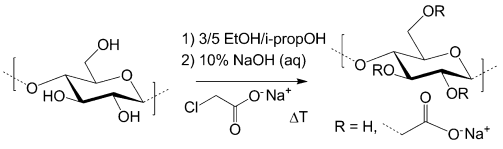

Fig. 2 Carboxymethylation of cellulose with chloroacetic acid

freeze-drying, vacuum drying or spray-drying) was necessary to obtain redispersible powders. However, some of the mentioned methods might also lead to redispersible CMC powders when the suspensions are dried from an alcohol mixture. As a second criterion, the DS must be high enough to prevent hornification during drying but sufficiently low to prevent solubilisation during water redispersion. Therefore, preliminary experiments were performed to select an appropriate DS that would satisfy the above requirements. Briefly, the selected experimental DS for RBP-mc (route 1) and RBP-cm (route 2) were 0.09 and 0.13, respectively.

To confirm successful carboxymethylation reaction, the powdered treated and untreated RBP were characterized using FT-IR spectroscopy (Fig. 3a). The spectrum of the untreated RBP showed the characteristic absorption bands of cellulose. A large band between 3,600 and 2,800 cm^{-1} contains CH stretching vibrations, and OH stretching vibrations from alcoholic groups and water. The broad band with a peak at 1,640 cm^{-1} was attributed to the bending vibrations of adsorbed water. A series of peaks between 1,500 and 1,300 cm^{-1} were associated to OCH deformation vibrations, CH_2 bending vibrations and CCH and COH bending vibrations. Finally, the band ranging from 1,200 to 900 cm^{-1} mainly contains the signals of CC stretching vibrations and COH and CCH deformation vibrations (Proniewicz et al. 2001). Mechanical disintegration of the RBP (RBP-m) did not lead to a change in the FT-IR spectrum. However, chemical modification of the RBP (RBP-mc, RBP-c and RBP-cm) led to the appearance of a new signal at 1,595 cm^{-1}, which was attributed to the asymmetric stretching vibration of the carboxylate group (Cuba-Chiem et al. 2008), confirming the successful carboxymethylation. As it can be observed, the intensity of the 1,595 cm^{-1} signal for the RBP-mc (route 1) is lower than those for the RBP-c and RBP-cm (route 2). This is in agreement with the experimental DS values previously reported where the DS for the RBP-mc was also lower than the one for the RBP-c.

CP-MAS ^{13}C-NMR was used to support the findings of the FT-IR experiments. Figure 3b shows the spectra of the untreated RBP and the treated RBP products of both routes in the region from 0 to 220 ppm. Also, an inset graph showing the region where the carboxylate signal appears (around

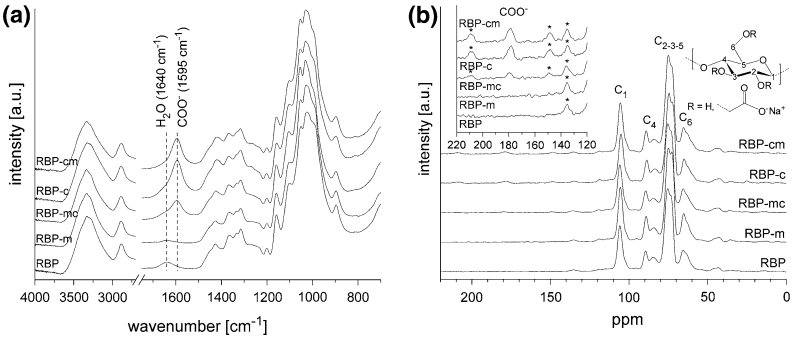

Fig. 3 **a** FT-IR and **b** ^{13}C CP-MAS NMR spectra of treated and untreated RBP

180 ppm) is included. Again, the RBP material shows the characteristic signal pattern of cellulose: C_1 (106 ppm), C_4 (90 and 85 ppm, from crystalline and amorphous domains, respectively), overlapped signals of C_2, C_3 and C_5 (between 70 and 80 ppm) and C_6 (66 ppm) (Gilardi et al. 1995; Kono et al. 2002). As expected, mechanical disintegration of RBP (RBP-m) did not promote changes in the chemical structure as all the NMR signals are identical. However, carboxymethylated RBP samples (RBP-mc, RBP-c and RBP-cm) showed a new signal at 180 ppm, which was attributed to the carboxylate group (Heinze and Koschella 2005). This peak is again more pronounced for the samples with higher DS, i.e. the RBP-c and the RBP-cm. Finally, the resonances marked with a star are spinning side bands of the carboxylate groups (210 and 150 ppm) and of the C_1 (136 ppm), respectively. Overall, the occurrence of the carboxymethylation reaction on the RBP samples was successfully evidenced by CT, FT-IR and CP-MAS ^{13}C-NMR analyses.

Chemical modification of cellulose can decrease its crystallinity (Sassi and Chanzy 1995) leading to a possible reduction of its reinforcing potential in composites with polymers. The effect of the mechanical and chemical treatments on the crystallinity of the different samples was analyzed by X-ray diffraction (Fig. 4a). The diffractogram of the untreated RBP shows reflections of the cellulose lattice planes appearing at 2θ angles between 13° and 17° ($1\bar{1}0$ and 110), 22.3° (020) and 34.5° (004) (Sassi and Chanzy 1995). The crystallinity χ_{cr} of the samples was estimated by using Eq. 1 (Segal et al. 1959) with I_{020} being the intensity of the 020 peak (amorphous and crystalline reflections at 22.3°) and I_{am} being the intensity of the minimum between the 020 and 110 peaks (amorphous reflections at 18.5°).

$$\chi_{cr} = \frac{I_{020} - I_{am}}{I_{020}}. \quad (1)$$

This method assumes that the amorphous part of the cellulose shows equal intensity at both 2θ angles, 18.5° and 22.3°, respectively. It also assumes that there is no portion of crystalline reflection at 18.5°. The highest value of crystallinity was obtained for RBP raw with 71%, followed by RBP-m (68%), RBP-mc (65%), RBP-c (63%) and RBP-cm (49%). As it can be observed, samples from route 1 (RBP-m and RBP-mc) showed very similar crystallinity values, implying that the crystalline structure was not significantly affected. However, samples from route 2 (RBP-c and RBP-cm), presented a more pronounced reduction in crystallinity. Consequently, mechanical disintegration had a stronger effect on crystallinity when the cellulose was carboxymethylated first. Apparently, the presence of the carboxylate groups makes the mechanical isolation more efficient, as not only amorphous parts but also crystalline domains are affected by the treatment. Increased efficiency for isolation of fibrillated material can be explained by ionic repulsion between the carboxylate groups of the single cellulose chains (Wågberg et al. 2008). Lower forces would therefore be sufficient to isolate the nanofibrillated material.

Another cause for reduction of the NFC reinforcing potential can be thermal degradation of NFC during compounding with polymers at high temperatures, i.e. by extrusion. Therefore, the thermal stability of the RBP samples was evaluated by TGA in dry gas nitrogen (Fig. 4b). As it can be observed,

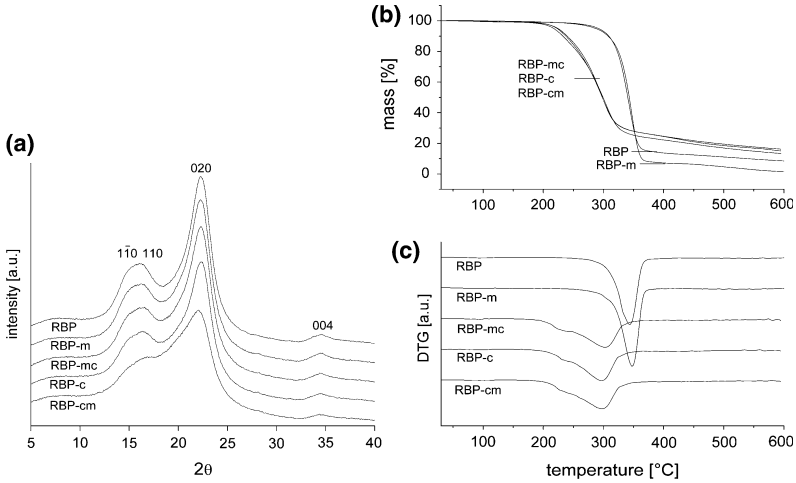

Fig. 4 **a** XRD diffractograms, **b** TGA spectra and **c** DTG spectra of treated and untreated RBP

the onset temperature of cellulose degradation was around 250 °C for the untreated RBP (top graph, weight loss curve) with a sharp degradation peak at 345 °C in the DTG (Fig. 4c, weight loss rate curve) at a heating rate of 20 °C/min. During the thermal degradation process, cellulose is converted into volatiles, tars and charcoal (Shafizadeh and McGinnis 1971). Mechanical disintegration of RBP (RBP-m) did not lead to significant changes in the characteristic degradation temperatures. However, chemical modification of the RBP (i.e. RBP-mc, RBP-c and RBP-cm) led to a decrease of both the onset degradation temperature and the degradation peak to 200 and 300 °C, respectively. Consequently, carboxymethylation clearly reduced the thermal stability of the studied products. This finding is in agreement with the results obtained from thermal degradation of TEMPO-mediated, oxidized cellulose (Fukuzumi et al. 2009) and of partially carboxymethylated cellulose (Lourdes-Leza et al. 1989).

The ability of the samples to form stable suspensions or gels in water was evaluated by qualitatively analyzing the sedimentation rate of the suspensions. Figure 5 shows testing tubes with 0.2% w/w (left series) and 1.0% w/w (right series) concentrations of redispersed RBP samples in water. After transferring the suspensions into the testing tubes, photographs were taken at 0 min, 15 min, 1 h and 20 h. At 0.2% concentration, complete sedimentation of the untreated RBP and the RBP-m occurred within 15 min and 1 h, respectively. In contrast, the suspensions of the carboxymethylated RBP suspensions (RBP-mc, RBP-c and RBP-cm) were stable for at least 1 h, with the RBP-cm being stable for the

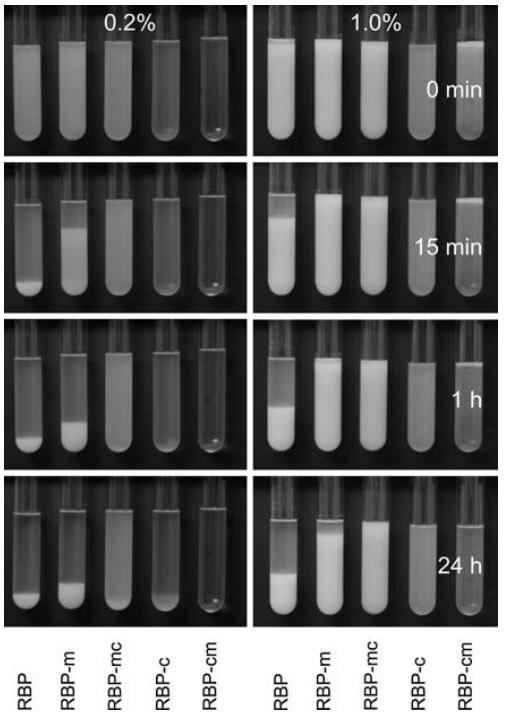

Fig. 5 Time-dependent sedimentation experiments of treated and untreated RBP in concentrations of 0.2 and 1.0%

whole studied period of time (i.e. 20 h). It should be noted that the stability of a carboxymethylated NFC suspension is susceptible to its pH and salt concentration (Wågberg et al. 2008). At 1.0% concentration, differences in the sedimentation behavior of the different RBP suspensions were more difficult to observe. However, differences in transparency of the suspensions became more distinct. Samples from route 1 (RBP-m and RBP-mc) formed a white suspension, whereas samples from route 2 (RBP-c and RBP-cm) were more transparent. The transparency of RBP-cm indicates that the dimensions of a major part of cellulose particles in the suspension were below the limit for light-scattering. This was verified by SEM characterization of the redispersed suspensions after freeze-drying (Fig. 6). The untreated RBP (a) formed large aggregates which were not dispersed in the suspension. This is in agreement with the much faster sedimentation rate of the RBP suspension compared to the other samples. RBP-m (b) did also form some aggregates, although they were smaller and some fibrils with diameters below the micrometer range remained isolated. Carboxymethylation of this sample (RBP-mc) did not lead to significant changes in the morphology of the freeze-dried cellulose. In contrast, RBP-c (d) formed a network of cellulose fibrils with overall diameters below 1 micron. The SEM image of

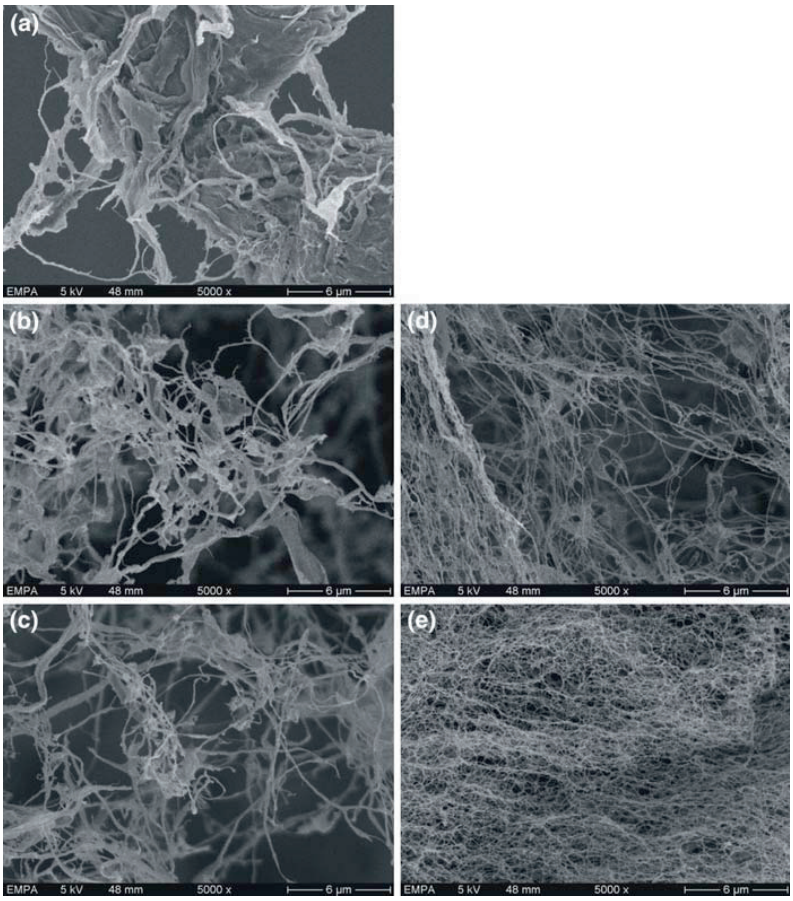

Fig. 6 SEM-images of water-redispersed and freeze-dried RBP samples at a magnification of ×5000, **a** RBP, **b** RBP-m, **c** RBP-mc, **d** RBP-c and **e** RBP-cm

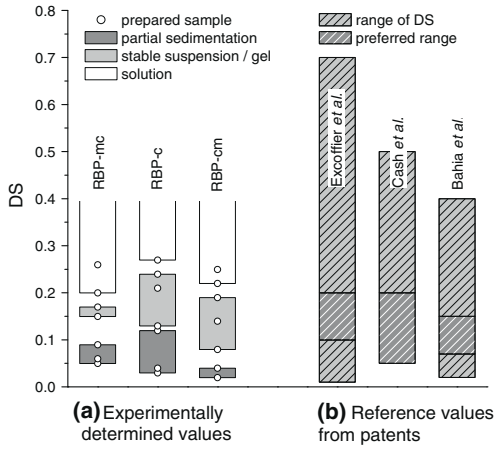

Fig. 7 **a** Appearance of treated RBP aqueous suspensions at 0.2% w/w compared with **b** the covered range of DS of carboxymethylated and mechanically disintegrated cellulose and the "preferred values" of DS, reported in patents

freeze-dried RBP-cm (e) showed a coherent system of cellulose nanofibrils, with overall diameters below 100 nm. The samples from route 2 (RBP-c and RBP-cm) showed clearly less agglomeration of the fibrils, which also were lower in diameter, compared to those of route 1 (RBP-m and RBP-mc). This also accounts for the increased stability of the suspensions from this route, as presented above.

The appearance of the redispersed CMC aqueous suspensions with respect to their DS is shown in Fig. 7a. A series of seven samples with varying DS was prepared for each carboxymethylated product (RBP-mc, RBP-c and RBP-cm). The various DS of the prepared powders are indicated by empty circles. The powders were dispersed in water at concentrations of 0.2% w/w and 1.0% w/w (data for 1.0% w/w not shown) and photographs were taken of the suspensions after 20 h (Fig. 8). The suspensions were then categorized into three classes, i.e. solutions (white), stable suspensions or gels (light grey) and suspensions showing partial sedimentation (dark grey). The suspensions with a concentration of 1.0% w/w were stable for the whole time range and no phase-separation or sedimentation was observed. However, at lower concentration (0.2% w/w), the differences between the samples became more evident: At low DS (between 0.05 and 0.09 for RBP-mc, 0.03 and 0.12 for RBP-c and 0.02 and 0.04 for RBP-cm) the translucent suspensions showed opaque, white sediments which were more pronounced in the RBP-c series. This partial sedimentation can be explained by local hornification due to the inhomogeneous substitution pattern at low substituted carboxymethyl celluloses (Walecka 1956). It is worth to note that pre-mechanical carboxymethylation (RBP-cm, route 2) seems to clearly reduce the level below

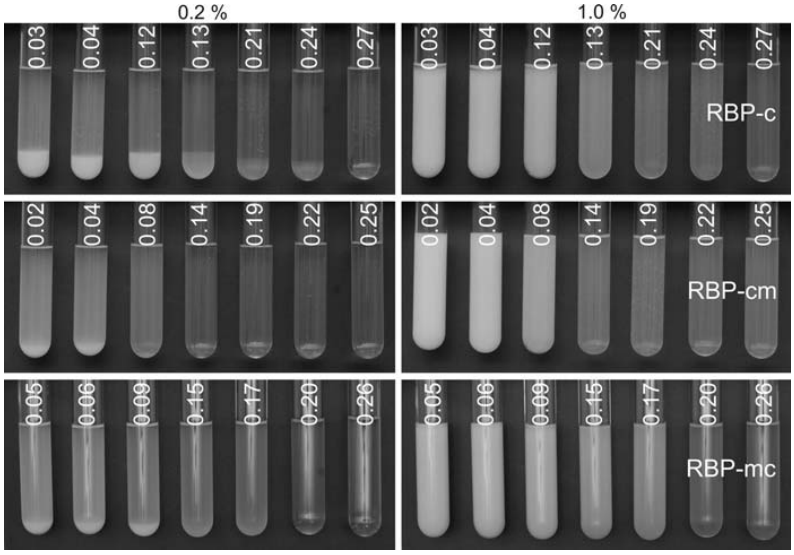

Fig. 8 Photographs of water-redispersed, treated RBP with various DS, at concentrations of 0.2 and 1.0% after 20 h

which hornification occurs. Also, it was reported that carboxymethylated, bleached sulfate pulp shows hornification below a DS of around 0.05 (Lindström and Carlsson 1982). At higher DS (between 0.15 and 0.17 for RBP-mc and 0.08 and 0.22 for RBP-cm) the suspensions were stable and almost transparent. Only the suspensions of RBP-c (between 0.13 and 0.24) showed some translucent sediments. Still, these suspensions were qualified as stable because of the small volumes and translucence of the sediments. Interestingly, the threshold DS above which the powders formed a solution were reduced for both products of the two routes. Pre-mechanical (RBP-cm, route 2) and post-mechanical (RBP-mc, route 1) carboxymethylation led to products which were soluble in water above a DS of 0.2 and 0.22, respectively. RBP-c was soluble above a DS of 0.27 which is close to the reported value of 0.3 Walecka (1956). Figure 7b shows the range of DS values covered for the preparation of redispersible carboxymethylated cellulose nanofibrils (light grey, striped) reported in patents (Excoffier et al. 1999; Cash et al. 2003 and Bahia 1995). In addition, the "preferred values" of DS indicated in the patents are highlighted (dark grey, striped). The experimentally determined range of DS to yield stable suspensions of water-redispersible, nanofibrillated cellulose in powder form coincides with the preferred values from the references.

Conclusions

Water-redispersible, nanofibrillated cellulose in powder form was prepared from refined, bleached beech pulp (RBP) by carboxymethylation (c) and mechanical disintegration (m). Two routes were examined, leading to four different products. In route 1, the RBP was mechanically disintegrated (RBP-m), followed by carboxymethylation (RBP-mc) with a DS of 0.09. In route 2, the sequence of the chemical and mechanical treatment was reversed, leading to the RBP-c and RBP-cm products with a DS of 0.13 and 0.14, respectively.

FT-IR and CP-MAS ^{13}C-NMR spectroscopy proved the occurrence of the carboxymethylation reaction of the RBP-mc, RBP-c and RBP-cm products with the appearance of characteristic signals for the carboxylate group at 1,595 cm^{-1} and 180 ppm, respectively. Also, mechanical disintegration of the RBP (RBP-m) did not lead to a change in chemical structure since the FT-IR and the ^{13}C solid state NMR spectra were identical.

XRD experiments showed a loss of crystallinity for the carboxymethylated samples, and this effect was especially pronounced for the products of route 2. Mechanical disintegration of the untreated RBP material did not significantly alter the crystalline structure. Also, TGA experiments evidenced a dramatic decrease in thermal stability of the carboxymethylated samples, since the onset temperature of the cellulose degradation dropped from 300 to 200 °C. This will limit the use of the final RBP products in nanocomposites to those biopolymers that do not require processing temperatures above 200 °C during extrusion.

On the other hand, SEM and sedimentation tests confirmed that carboxymethylation was essential to obtain water-redispersible powders, capable of forming stable suspensions. Specifically, samples that were first carboxymethylated (those from route 2) formed a more transparent suspension in water and showed a more homogeneous network with overall diameters below 1 μm (RBP-c and RBP-cm). Mechanical disintegration of the RBP (RBP-m) improved dispersibility in water compared to the untreated RBP but it was not very stable as it phase-separated with time.

These results demonstrate that the water-redispersible RBP powders obtained in this work are an attractive alternative to the conventional nanofibrillated cellulose aqueous suspensions as starting material for the synthesis of novel cellulose nanocomposites. The powdered chemically modified RBP would not only allow reducing storage volume and shipping costs but also they would increase the storage life of the product against bacterial degradation. Furthermore, the generated carboxylate groups on the surface of the derivatized RBP could undergo further chemical modification (e.g. esterification) to enhance the chemical affinity of the fibrils to a specific non-polar matrix.

Acknowledgments The authors wish to express their thanks to Beatrice Fischer, as well as Urs Gfeller and Dr. Peter Lienemann for performing the TGA and XRD measurements, respectively and Dr. Philippe Tingaut for carefully reading the manuscript. The authors gratefully acknowledge the State Secretariat for Education and Research (SER) for financial support of this work.

References

Abe K, Iwamoto S, Yano H (2007) Obtaining cellulose nanofibers with a uniform width of 15 nm from wood. Biomacromolecules 8:3276–3278

Andresen M, Johansson LS, Tanem BS, Stenius P (2006) Properties and characterization of hydrophobized microfibrillated cellulose. Cellulose 13:665–677

Araki J, Wada M, Kuga S (2001) Steric stabilization of a cellulose microcrystal suspension by poly(ethylene glycol) grafting. Langmuir 17:21–27

Bahia HS (1995) Treatment of cellulose. Patent publication number WO9515342

Boldizar A, Klason C, Kubat J (1987) Prehydrolyzed cellulose as reinforcing filler for thermoplastics. Int J Polym Mater 11:229–262

Bordeanu N, Eyholzer Ch, Zimmermann T (2008) Cellulose nanostructures with tailored functionalities. Pending patent

Cantiani R, Guerin G, Senechal A, Vincent I, Benchimol J (2001) Patent publication numbers US6224663, US6231657, US6306207

Cash MJ, Chan AN, Conner HT, Cowan PJ, Gelman RA, Lusvardi KM, Thompson SA, Tise FP (2003) Derivatized microfibrillar polysaccharide. Patent publication number WO0047628

Chakraborty A, Sain M, Kortschot M (2006) Reinforcing potential of wood pulp-derived microfibres in a PVA matrix. Holzforschung 60:53–58

Couderc S, Ducloux O, Kim BJ, Someya T (2009) A mechanical switch device made of a polyimide-coated microfibrillated cellulose sheet. J Micromech Microeng 19:055006

Cuba-Chiem LT, Huynh L, Ralston J, Beattie DA (2008) In situ particle film ATR FTIR spectroscopy of carboxymethyl cellulose adsorption on talc: binding mechanism, pH effects, and adsorption kinetics. Langmuir 24:8036–8044

Dinand E, Chanzy H, Vignon M, Maureaux A, Vincent I (1996) Microfibrillated cellulose and method for preparing same from primary wall plant pulp, particularly sugar beet pulp. Patent publication number WO9624720

Excoffier G, Vignon M, Benchimol J, Vincent I, Hannuksela T, Chauve V (1999) Parenchyma cellulose substituted with carboxyalkyl groups and preparation method. Patent publication number WO9938892

Eyler RW, Klug ED, Diephuis F (1947) Determination of degree of substitution of sodium carboxymethylcellulose. Anal Chem 19:24–27

Fukuzumi H, Saito T, Iwata T, Kumamoto Y, Isogai A (2009) Transparent and high gas barrier films of cellulose nanofibers prepared by TEMPO-mediated oxidation. Biomacromolecules 10:162–165

Gilardi G, Abis L, Cass AEG (1995) Carbon-13 CP/MAS solid-state NMR and FT-IR spectroscopy of wood cell wall biodegradation. Enzyme Microb Technol 17:268–275

Goussé C, Chanzy H, Cerrada ML, Fleury E (2004) Surface silylation of cellulose microfibrils: preparation and rheological properties. Polymer 45:1569–1575

Heinze T, Koschella A (2005) Carboxymethyl ethers of cellulose and starch—a review. Macromol Symp 223:13–39

Herrick FW (1984) Process for preparing microfibrillated cellulose. Patent publication number US4481077

Herrick FW, Casebier RL, Hamilton JK, Sandberg KR (1983) Microfibrillated cellulose: morphology and accessibility. J Appl Polym Sci: Appl Polym Symp 37:797–813

Hubbe MA, Rojas OJ, Lucia LA, Sain M (2008) Cellulosic nanocomposites: a review. Biores 3:929–980

Hult EL, Larsson PT, Iversen T (2001) Cellulose fibril aggregation—an inherent property of kraft pulps. Polymer 42:3309–3314

Kono H, Yunoki S, Shikano T, Fujiwara M, Erata T, Takai M (2002) CP/MAS ^{13}C NMR study of cellulose and cellulose derivatives. 1. Complete assignment of the CP/MAS ^{13}C NMR spectrum of the native cellulose. J Am Chem Soc 124:7506–7511

Laivins GV, Scallan AM (1993) The mechanism of hornification of wood pulps. In: Proc 10th fundamental research sympoisum. Oxford, pp 1235–1260

Lasseuguette E (2008) Grafting onto microfibrils of native cellulose. Cellulose 15:571–580

Lindström T, Carlsson G (1982) The effect of carboxyl groups and their ionic form during drying on the hornification of cellulose fibers. Svensk Papperstidning 85:R146–R151

Lourdes-Leza M, Cortazar M, Casinos I, Guzmán GM (1989) Thermal degradation of partially carboxymethylated cellulose grafted with 4-vinylpyridine. Angew Makromol Chem 168:195–203

Pääkkö M, Ankerfors M, Kosonen H, Nykänen A, Ahola S, Österberg M, Ruokolainen J, Laine J, Larsson PT, Ikkala O, Lindström T (2007) Enzymatic hydrolysis combined with mechanical shearing and high-pressure homogenization for nanoscale cellulose fibrils and strong gels. Biomacromolecules 8:1934–1941

Proniewicz LM, Paluszkiewicz C, Weselucha-Birczyńska A, Majcherczyk H, Barański A, Konieczna A (2001) FT-IR and FT-Raman study of hydrothermally degradated cellulose. J Mol Struct 596:163–169

Reid JD, Daul GC (1947) The partial carboxymethylation of cotton to obtain swellable fibers, I. Text Res J 17: 554–561

Saito T, Nishiyama Y, Putaux JL, Vignon M, Isogai A (2006) Homogeneous suspensions of individualized microfibrils from TEMPO-catalyzed oxidation of native cellulose. Biomacromolecules 7:1687–1691

Sassi JF, Chanzy H (1995) Ultrastructural aspects of the acetylation of cellulose. Cellulose 2:111–127

Scallan AM, Tigerström AC (1992) Swelling and elasticity of the cell walls of pulp fibres. J Pulp Pap Sci 18:188–193

Segal L, Creely JJ, Martin AE Jr, Conrad CM (1959) An empirical method for estimating the degree of crystallinity of native cellulose using the X-Ray diffractometer. Text Res J 29:786–794

Shafizadeh F, McGinnis GD (1971) Chemical composition and thermal analysis of cottonwood. Carbohydr Res 16: 273–277

Stenstad P, Andresen M, Tanem BS, Stenius P (2008) Chemical surface modifications of microfibrillated cellulose. Cellulose 15:35–45

Turbak AF, Snyder FW, Sandberg KR (1983) Microfibrillated cellulose, a new cellulose product: properties, uses, and commercial potential. J Appl Polym Sci: Appl Polym Symp 37:815–823

Wågberg L, Winter L, Ödberg L, Lindström T (1987) On the charge stoichiometry upon adsorption of a cationic polyelectrolyte on cellulosic materials. Colloid Surfaces 27:163–173

Wågberg L, Decher G, Norgren M, Lindström T, Ankerfors M, Axns K (2008) The build-up of polyelectrolyte multilayers of microfibrillated cellulose and cationic polyelectrolytes. Langmuir 24:784–795

Walecka JA (1956) An investigation of low degree of substitution carboxymethylcelluloses. Tappi 39:458–463

Yano H, Nakahara S (2004) Bio-composites produced from plant microfiber bundles with a nanometer unit web-like network. J Mater Sci 39:1635–1638

Yano H, Sugiyama J, Nakagaito AN, Nogi M, Matsuura T, Hikita M, Handa K (2005) Optically transparent composites reinforced with networks of bacterial nanofibers. Adv Mater 17:153–155

Young RA (1994) Comparison of the properties of chemical cellulose pulps. Cellulose 1:107–130

Zadorecki P, Michell AJ (1989) Future-prospects for wood cellulose as reinforcement in organic polymer composites. Polym Compos 10:69–77

Paper II

Cellulose (2010) 17:387–398
DOI 10.1007/s10570-010-9396-8

DMA analysis and wood bonding of PVAc latex reinforced with cellulose nanofibrils

Francisco López-Suevos · Christian Eyholzer · Nico Bordeanu · Klaus Richter

Received: 4 September 2009 / Accepted: 2 January 2010 / Published online: 16 January 2010

Abstract Suspensions of commercial refined beech pulp (RBP) were further processed through mechanical disintegration (MD-RBP), chemical modification (CM-RBP) and through chemical modification followed by mechanical disintegration (CM-MD-RBP). Nanocomposites were prepared by compounding a poly(vinyl acetate) (PVAc) latex adhesive with increasing contents of the different types of nanofibrils, and the resulting nanocomposites were analyzed by dynamic mechanical analysis (DMA). Also, the suitability of using the CM-RBP fibrils to formulate PVAc adhesives for wood bonded assemblies with improved heat resistance was studied. The presence of cellulose nanofibrils had a strong influence on the viscoelastic properties of PVAc latex films. For all nanocomposites, increasing amounts of cellulose nanofibrils (treated or untreated) led to increasing reinforcing effects in the glassy state, but especially in the PVAc and PVOH glass transitions. This reinforcement primarily resulted from interactions between the cellulose fibrils network and the hydrophilic PVOH matrix that led to the complete disappearance of the PVOH glass transition (tan δ peak) for some fibril types and contents. At any given concentration in the PVOH transition, the CM-MD-RBP nanofibrils provided the highest reinforcement, followed by the MD-RBP, CM-RBP and the untreated RBP. Finally, the use of the CM-RBP fibrils to prepare PVAc reinforced adhesives for wood bonding was promising since, even though they generally performed worse in dry and wet conditions, the boards showed superior heat resistance (EN 14257) and passed the test for durability class D1.

Keywords Cellulose nanofibrils · Carboxymethylation · Mechanical disintegration · PVAc latex · Reinforcement · DMA · Wood bonding

F. López-Suevos (✉) · C. Eyholzer · N. Bordeanu · K. Richter
Empa, Swiss Federal Laboratories for Materials Testing and Research, Wood Laboratory Überlandstrasse 129, 8600 Dübendorf, Switzerland
e-mail: Fuco.lopezsuevos@gmail.com

F. López-Suevos
Centro de Innovación e Servizos Tecnolóxicos da Madeira de Galicia, CIS-Madeira, Avda. de Galicia, n°5, Parque Tecnolóxico de Galicia, 32901 San Cibrao das Viñas, Spain

C. Eyholzer
Division of Manufacturing and Design of Wood and Bionanocomposites, Luleå University of Technology (LTU), Luleå, Sweden

Introduction

Cellulose nanofibrils (CNF) derived from biomass resources are increasingly being used as reinforcing agents in the preparation of nanocomposites with polymer matrices due to their interesting properties, such as high strength and stiffness (Hubbe et al. 2008;

Yano and Nakahara 2004; Zadorecki and Michell 1989), transparency (Yano et al. 2005) or biodegradability (Couderc et al. 2009). Although CNF have been proved suitable to prepare nanocomposites with apolar matrices after chemical modification (e.g. silylation, TEMPO oxidation, acetylation or reactions with anhydrides) of the surface hydroxyl groups (Andresen et al. 2006; Araki et al. 2001; Goussé et al. 2004; Lasseuguette 2008; Saito et al. 2006; Sassi and Chanzy 1995; Stenstad et al. 2008), the hydrophilic nature of CNF makes them especially attractive for polar matrices such as PVOH (Zimmermann et al. 2005; Roohani et al. 2008; Lu et al. 2008), hydroxypropyl cellulose (Zimmermann et al. 2005), acrylic and phenol–formaldehyde resins (Iwamoto et al. 2007; Nakagaito and Yano 2004, 2005, 2008), or poly(styrene-co-butyl acrylate) (Samir et al. 2004; Dalmas et al. 2007) and PVAc (De Rodriguez et al. 2006) latexes. However, the main drawback of using the hydrophilic CNF is that they have to be stored as aqueous suspensions (10–30 wt%) since irreversible agglomeration of the fibrils through hydrogen bonding will occur during drying, i.e. hornification (Young 1994; Hult et al. 2001). Fortunately, partial carboxymethylation of the CNF is well-known to prevent hornification (Bordeanu et al. 2008; Cantiani et al. 2001a, b, c; Cash et al. 2000; Eyholzer et al. 2009; Dinand et al. 1996; Excoffier et al. 1999; Herrick 1984; Laivins and Scallan 1993; Lindström and Carlsson 1982), and consequently, carboxymethylated CNF (highly hydrophilic) can be obtained in powder form that is water-redispersible. Finally, in addition to adequate fibril/matrix chemical affinity, attainable reinforcement levels are closely related to the degree of mechanical disintegration of the fibrils. Therefore, the mechanical properties of nanocomposites can be modified by properly processing and refining the CNF (Zimmermann et al. 2004).

The mechanical properties of nanocomposites can be efficiently evaluated by dynamic mechanical thermal analysis (DMA) as a function of time/frequency and temperature. Moreover, DMA is especially suited to identify fibril/matrix interactions or changes in the viscoelastic properties of nanocomposites in the glassy, glass transition and rubbery plateau regions. For instance, Lu et al. (2008) showed that increasing amounts of microfibrillated cellulose (derived from kraft pulp) to a PVOH matrix led to a significant increase of the storage modulus in the glassy region and especially in the rubbery plateau. Kvien and Oksman (2007) reported a significant difference in storage modulus in the glassy region of a PVOH matrix when using cellulose nanowhiskers (CNW) oriented in parallel or transverse directions. Dalmas et al. (2007) showed that cellulose nanofibrils obtained from sugar beet pulp provided a large mechanical reinforcement to an amorphous poly(styrene-co-butyl acrylate) matrix in the rubbery plateau region. This effect was explained by the formation of a rigid nanofibril network through hydrogen bonding, which was governed by a percolation mechanism (Azizi Samir et al. 2005). Alemdar and Sain (2008) showed the reinforcing effect of wheat straw cellulose nanofibers in a starch-based thermoplastic polymer (TPS). Interestingly, the presence of the nanofibers remarkably shifted the neat TPS glass transition temperature (Tg) 30–40 °C, which was attributed to interfacial TPS/nanofibers interactions. Similarly, Kristo and Biliaderis (2007) attributed the significant increase in the sorbitol-plasticized pullulan Tg with increasing amounts of starch nanocrystals to strong filler/filler and filler/polymer interactions. In summary, these studies demonstrate the potential of the DMA technique to identify fibril/polymer interactions and to evaluate reinforcement effects in the viscoelastic response of cellulose nanocomposites.

In the present work, the aqueous RBP suspensions were further processed through chemical modification (CM-RBP), mechanical disintegration (MD-RBP) and through chemical modification followed by mechanical disintegration (CM-MD-RBP). Nanocomposites were prepared by mixing a commercial PVAc latex with different concentrations of the untreated or the processed RBP fibrils. The resulting nanocomposites were analyzed by DMA to investigate the influence of the different types of cellulose nanofibrils on the PVAc viscoelastic properties and to identify possible fibril/PVAc interactions. Finally, the suitability of the CM-RBP fibrils to prepare PVAc adhesives intended for wood bonded assemblies with enhanced heat resistance was evaluated.

Materials and methods

Materials

The refined, bleached beech pulp (RBP) was provided by J. Rettenmaier & Söhne GmbH, Rosenberg,

Germany (Arbocel B1011, 10 wt% aqueous suspension. The chloroacetic acid (sodium salt, purity ≥ 98%) and the glacial acetic acid (purity ≥ 99.8%) were purchased from Merck (Darmstadt, Germany), and the sodium hydroxide (NaOH, purity ≥ 98%) from Fluka (Buchs, Switzerland).

The commercial PVAc latex used was VN 1693 (Collano AG, Switzerland) with a solids content of 49.5 ± 0.1%. This system is an aqueous suspension of PVAc particles stabilized by PVOH and it does not contain cross-linking agents. This is a thermoplastic wood adhesive for non-structural applications classified as suitable for durability class D3 (EN 204:2001) by the provider. Briefly, durability class 3 implies that the bonded member can be used in interior with frequent short-term exposure to running or condensed water and/or to heavy exposure to high humidity. Also, it can be used in exterior not exposed to weather.

Mechanical disintegration

About 1.40 kg of the RBP aqueous suspension (ca. 10 wt%) were initially mixed with 8 L of water and stirred with a stainless steel agitator for 30 min at 20 °C in a 10 L reactor. The diluted RBP suspension (ca.1.5 wt%) was then processed with an inline disperser (Megatron MT 3000, Kinematica AG, Switzerland) at 20,000 rpm for 60 min. This pretreatment facilitated the breaking down of the RBP fibrous material into smaller parts (cellulose fibril bundles) providing a more homogeneous suspension. Then, 6 L of the pretreated RBP suspension were subjected to high-shear disintegration in a Microfluidizer type M-110Y (Microfluidics Corporation, USA). A stable cellulose nanofibril suspension (MD-RBP) was obtained after 6 passes through the $H230Z_{400\ \mu m}$ and $F20Y_{75\ \mu m}$ interaction chambers of the microfluidizer. The estimated processing pressure inside the F20Y chamber was 125 MPa.

Chemical modification

About 2.54 kg of the 10 wt% RBP aqueous suspension were transferred to a 10 L reactor equipped with the inline disperser and a mechanical stirrer, and then 7.46 kg of a 5/3 v/v isopropanol/ethanol mixture were added. The resulting mixture was processed with the inline disperser at 15,000 rpm for 30 min at 20 °C followed by slow addition of 189.50 g of a 21 wt% sodium hydroxide aqueous solution under continuous stirring to activate the cellulose. Then, 115.02 g of chloroacetic acid (sodium salt) were added to the activated suspension and the temperature was increased to 60 °C. The reaction mixture was again processed with the inline disperser at 20,000 rpm for 2 h before cooling it down to 20 °C to stop the reaction. The resulting suspension was neutralized with acetic acid and centrifuged at 15,000 rpm for 90 min. The supernatant was discarded and the precipitate containing the carboxymethylated cellulose fibrils was washed first with distilled water three times to remove any water-soluble by-product and second with a 5/3 v/v isopropanol/ethanol mixture prior to drying overnight in the oven at 65 °C. The resulting powdered CM-RBP fibrils are easily re-dispersable in water forming a stable gel. The degree of substitution (DS) of the CM-RBP was evaluated by conductometric titration according to a modified method from Eyler et al. (1947) and described in a previous study (Eyholzer et al. 2009). A DS of 0.156 ± 0.028 was obtained from three independent evaluations, which amounts to 5.2% of the hydroxyl groups present in the cellulose fibrils being replaced by carboxyl groups. As a reference, when the DS of the CM-RBP is greater than 0.25 the cellulose fibrils become soluble in water (Eyholzer et al. 2009).

Finally, the CM-MD-RBP fibrils were prepared by initially re-dispersing 69.2 g of the dry CM-RBP in 2.69 kg of water (ca. 2.5% by weight) with a high-shear blender (Ultra-Turrax, IKA, Germany). The resulting suspension was then transferred to the 10 L reactor and the mechanical disintegration treatment was conducted as previously described.

Preparation of nanocomposites

Composites were prepared by mixing the PVAc latex with the RBP, MD-RBP, CM-RBP or CM-MD-RBP fibrils at different concentrations, i.e. 5, 10, 20 and 30 wt% (g of dry fibrils in 100 g of total dry material). The PVAc-fibrils mixtures were blended with the Ultra-Turrax and degassed under vacuum before casting the films onto silicon molds. The films were dried under ambient conditions for 2 days and then cut with a twin-bladed cutter to obtain 45 (length) × 10 (width) × 0.6–0.7 (thickness) mm samples. Prior to

DMA analysis, all samples were dried by storage over silica gel under vacuum for at least 3 days.

Field emission scanning electron microscopy

The surface of the PVAc nanocomposites (previously dried as described for the DMA samples) with 10 and 30 wt% of the CM-MD-RBP fibrils were evaluated on a Jeol 6300F FE-SEM (Jeol Ltd., Japan) instrument. For the preparation of the FE-SEM samples, glimmer plates bonded to the sample's holder with a conducting carbon paste were employed. The samples were placed on the glimmer plates, and then coated with a platinum layer of 9 nm (*BAL-TEC MED 020* modular high vacuum coating system, BAL-TEC AG, Principality of Liechtenstein). The FE-SEM experiments were conducted at an accelerating voltage of 5 kV.

DMA experiments

A GABO-Eplexor DMA 800 (GABO qualimeter Testanlagen GmbH, Germany) in tension mode was used to study the viscoelastic properties of the resulting dried PVAc nanocomposites. All samples were initially conditioned at 0 °C for 5 min in the DMA, and then dynamic heating scans were performed from 0 to 150 °C at 2 °C/min and 10 Hz. The contact force, the static load strain and the dynamic load strain used in these experiments were 0.1 N, 0.3 and 0.03%, respectively. Three analyses were obtained for each sample.

Assessment of adhesive performance

Three adhesive formulations, namely, the neat PVAc and the PVAc with 1 and 3 wt% of the CM-RBP were selected to prepare three bonded panels of $1000 \times 135 \times 10$ mm^3 using beech wood ($10.8 \pm 0.5\%$ moisture content, $n = 10$). The preparation details of the bonded assemblies with these three adhesives are shown in Table 1. Each panel was cut into individual test specimens of $150 \times 20 \times 10$ mm according to EN 205:2003. The resulting 30 lap joint test pieces per board were randomly distributed into three treatment groups (Table 2): (1) 10 specimens were conditioned at (20 ± 2) °C and $(65 \pm 5)\%$ relative humidity for 7 days (Standard atmosphere or durability class D1, EN 204:2001), (2) 10 specimens were conditioned in the above standard atmosphere followed by 4 days in water at (20 ± 5) °C (Durability class D3, EN 204:2001) and (3) 10 specimens were conditioned in the described standard atmosphere and then each test piece was heated for 1 h in a preheated fan oven at 80 °C (WATT '91 test) according to EN 14257:2006. Immediately after each treatment, the specimens were tested in a Universal Testing Machine (Zwick 1474, Zwick GmbH & Co. KG, Germany) to evaluate the tensile shear strength parallel to the grain.

Table 1 Preparation of Beech bonded assemblies with three PVAc formulations

Boards	1	2	3
Adhesive	PVAc	PVAc with 1% CM-RBP	PVAc with 3% CM-RBP
Solids content (%)[a,c]	49.5 ± 0.1	46.0 ± 0.2	40.8 ± 0.2
Apparent viscosity[b,c] (Pa.s)	9.55 ± 0.07	3.16 ± 0.02	3.83 ± 0.01
Spreading rate[d] (g/m^2)		185[f]	
Open time (min)[e]		5[f]	
Pressure (N/mm^2)		0.3[f]	
Press time (h)		2[f]	
Press temperature (° C)		20–21[f]	

[a] Determined according to ASTM D 1489-87

[b] Measurement at 14.38 s^{-1} and 20 °C using a cone (40 mm, 1.59°)/plate in a Physica MCR 300 rheometer

[c] Average value for three samples with standard deviation

[d] Amount and application is on each bonding surface

[e] Time elapsing from adhesive application to assembly of the lamellas

[f] The same value was used for the three adhesive formulations

Table 2 Conditioning treatments for the lap joint test pieces and minimum required tensile shear strength values

Treatment	Duration and condition	Shear strength (N/mm^2)	European standard
Durability class D1	7 days in standard atmosphere[a]	≥10	EN 204 and 205
Durability class D3	7 days in standard atmosphere[a]	≥2	EN 204 and 205
	4 days in water at (20 ± 5) °C		
WATT ′91	7 days in standard atmosphere[a]	Not specified[b]	EN 14257
	(60 ± 2) min at (80 ± 2) °C		

[a] (20 ± 2) °C and (65 ± 5)% relative humidity

[b] In general, there is not specific requirement; only when the adhesive is intended for window sections a shear strength higher than 7 N/mm^2 is required

The rate of separation of the jaws was 50 mm/min for all samples. Specifically for the WATT ′91 test, the time between removal of the test piece from the oven and the start of the test has to be 9 ± 1 s.

Additionally, the steady-state flow properties of these liquid PVAc adhesives were measured in order to find out the influence of the CM-RBP fibrils on the PVAc rheological behaviour. These experiments were conducted in a Physica MCR 300 rheometer at 20 °C using a cone (40 mm, 1.59°)/plate from 100 to 1 s^{-1} of shear rate. The resulting flow curves were fitted to the Power law equation ($\tau_{zx} = k\,(dVz/dx)^n$), where τ_{zx} is the shear stress (Pa), (dVz/dx) is the shear rate (s^{-1}), k is the consistency index ($Pa.s^n$) and n is the power law index (Fig. 1). The fit was conducted collectively on three data sets from the respective sample types and the goodness of fit (R^2) was always higher than 0.99.

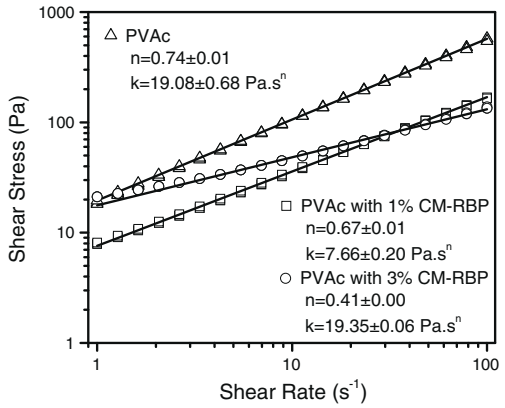

Fig. 1 Flow curves of the three liquid PVAc adhesives fitted to the Power law equation (*solid lines*) showing the consistency (k) and the power law (n) indexes. The fit was conducted collectively on three data sets from the respective sample types and the goodness of fit (R^2) was always higher than 0.99

Statistical analysis

One-way analysis of variance (ANOVA) was performed on the shear strength data for each treatment, with the adhesive type as independent variable. Tukey multiple comparison tests were conducted if a significant difference ($p \leq 0.05$) existed. Version 2.03 of the Windows SigmaStat software was used to conduct this statistical analysis.

Results and discussion

Figures 2 and 3 show the evolution of the storage modulus (top graphs) and tan δ (bottom graphs) with temperature for the PVAc nanocomposites prepared with the the RBP and CM-RBP (Fig. 2), and MD-RBP and CM-MD-RBP (Fig. 3) fibrils at different concentrations (i.e. 0, 5, 10, 20 and 30 wt%). All graphs show the same temperature, storage modulus and tan δ scales in order to facilitate comparisons between nanocomposites. Also, inset graphs of the storage modulus response in the low temperature region are provided to help visualize differences. The reproducibility of the viscoelastic response was very good, as demonstrated by the nearly perfect overlap of three repeat curves for each sample type. Spanning from low to high temperatures, three different regions can be identified in the neat PVAc films (open circle symbols): the glassy state (approx. below 25 °C), the PVAc glass transition (25–65 °C) (López-Suevos and Frazier 2005; Backman and Lindberg 2004) with a tan δ peak near 45 °C, and the very broad PVOH glass transition (65–150 °C) (López-Suevos and

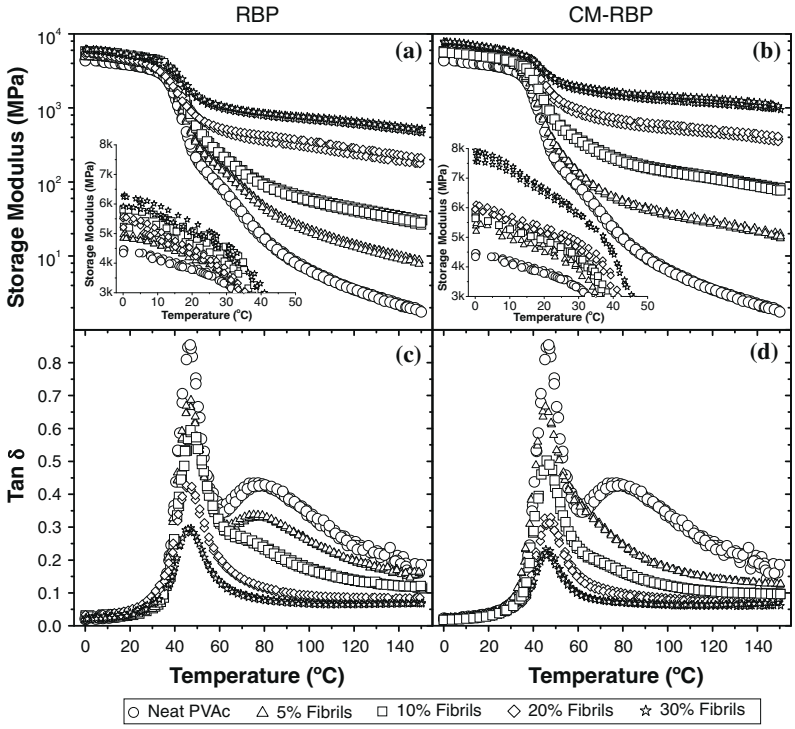

Fig. 2 Dynamic heating scans showing the storage modulus (*top graphs*) and tan δ (*bottom graphs*) for PVAc composites prepared with the RBP and CM-RBP cellulose fibrils at 0, 5, 10, 20 and 30 wt%. Three repetitions at each concentration are shown. *Insets* show expanded plot of the storage moduli in the low temperature region (glassy region)

Frazier 2006) with a tan δ peak around 80 °C. As the temperature increased through these two glass transitions the neat films dramatically softened, as showed by the almost four decade reduction in storage modulus.

First of all, it should be highlighted that the presence of the cellulose nanofibrils had a remarkable effect on the viscoelastic properties of the resulting nanocomposites, regardless of the fibril type (treated or untreated) and content. This was demonstrated by an increase in their storage modulus in the whole temperature range and a decrease in the tan δ intensity above the PVAc glassy state (Figs. 2, 3). We defined a reinforcement factor, RF, calculated by dividing the storage modulus for each composite by the storage modulus of the neat PVAc at the same temperature, i.e. the RF is the number of times the storage modulus was increased by the presence of the fibrils (Table 3). When considering the glassy region (see inset graphs of Figs. 2, 3 or Table 3, column for 0 °C), the storage modulus moderately increased with increasing loadings of each type of cellulose nanofibrils (RF values ranging from 1.11 to 1.39 for the RBP, 1.21 to 1.76 for the CM-RBP, 1.12 to 1.57 for the MD-RBP and 1.15 to 1.64 for the CM-MD-RBP nanocomposites). Interestingly, when the different fibrils were compared at the same concentrations, the reinforcement provided by the untreated RBP fibrils was quite similar to that of the treated fibrils (CM-RBP, MD-RBP and CM-MD-RBP) at 5 and 10 wt% but markedly smaller at 20 and 30 wt% (Table 3, column for 0 °C).

In the PVAc glass transition, on the one hand, the presence of cellulose fibrils did not significantly alter the PVAc glass transition temperature (±2 °C from tan δ peak) suggesting, according to similar studies (Backman and Lindberg 2004), a weak interaction between the bulk PVAc particles and the fibrils. Indeed, since PVAc is hydrophobic, it seems very unlikely that the fibrils would penetrate into a neat

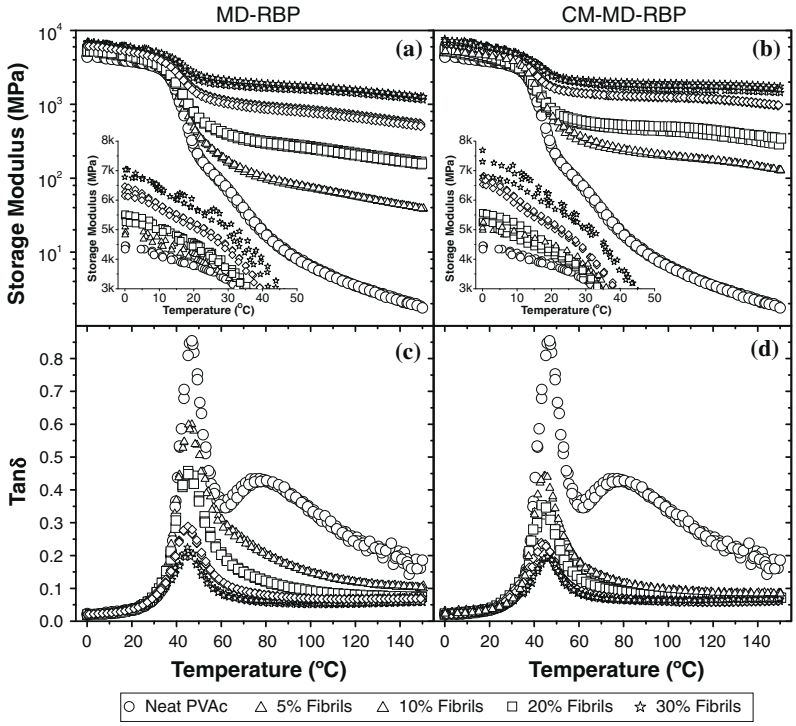

Fig. 3 Dynamic heating scans showing the storage modulus (*top graphs*) and tan δ (*bottom graphs*) for PVAc composites prepared with the MD-RBP and CM-MD-RBP cellulose nanofibrils at 0, 5, 10, 20 and 30 wt%. Three repetitions at each concentration are shown. *Insets* show expanded plot of the storage moduli in the low temperature region (glassy region)

PVAc region. On the other hand, the storage modulus in the PVAc glass transition significantly increased up to nearly 1.5 decades and the damping intensity (tan δ peak) decreased from 0.85 to 0.19, depending on the fibril type and concentration (maximum storage modulus and minimum tan δ intensity were obtained when using 30 wt% of the CM-MD-RBP).

Even more significant was the effect of the fibrils in the PVOH glass transition, which led to increases in the storage modulus of up to three decades with respect to the neat PVAc films (Figs. 2, 3). For each type of fibril, the RF values dramatically increased, especially at 150 °C, with increasing fibril contents. For example, the RF varied (at 150 °C) from 6.6 to 494 for the RBP, 17 to 1001 for the CM-RBP, 37 to 1208 for the MD-RBP, and 126 to 1588 for the CM-MD-RBP nanocomposites. More interestingly, the presence of the fibrils also led to the gradual disappearance of the tan δ peak with increasing fibril contents (Figs. 2, 3). These effects are associated with the segmental motions of the PVOH chains being increasingly restricted by the presence of the nanofibrils network and their strong interaction with the highly hydrophilic PVOH. Also, because of chain transfer reactions during polymerization of the PVAc, it is very likely that PVOH is covalently bonding the particle surfaces acting much like a capsular barrier. Because of this, the reinforcement observed in the PVAc glass transition might also be attributed to these strong PVOH/fibril interactions and possibly to fibril/fibril interactions (within the PVOH matrix) at the particle boundaries. Since PVOH is dispersed around the PVAc particles, it is clear that effects at the PVOH-rich boundaries will have an impact on the PVAc bulk particles. Supporting this mechanism, SEM images from nanocomposites with 10 and 30 wt% of CM-MD-RBP (Fig. 4) showed that cellulose nanofibrils mostly form a compact network covering the surface of the PVAc particles and the interparticle regions. They also showed some isolated cellulose

Table 3 Storage modulus and reinforcement provided by the differently treated cellulose fibrils (chemical, mechanical or both) at different concentrations at 0, 80 and 150 °C

PVAc nanocomposite	0 °C		80 °C		150 °C	
	Storage modulus (MPa)	Reinforcement factor[a]	Storage modulus (MPa)	Reinforcement factor[a]	Storage modulus (MPa)	Reinforcement factor[a]
Neat PVAc	4417 (67)	1	17 (0)	1	1.8 (0.1)	1
5% RBP	4900 (60)	1.11 (0.02)	44 (1)	2.6 (0.1)	8.4 (0.6)	4.6 (0.4)
5% CM-RBP	5347 (133)	1.21 (0.04)	56 (2)	3.3 (0.1)	19 (1)	10 (1)
5% MD-RBP	4940 (138)	1.12 (0.04)	99 (5)	5.9 (0.3)	39 (1)	21 (1)
5% CM-MD-RBP	5097 (139)	1.15 (0.04)	242 (8)	14 (1)	128 (1)	70 (3)
10% RBP	5543 (293)	1.26 (0.07)	93 (2)	5.5 (0.2)	29 (2)	16 (1)
10% CM-RBP	5717 (100)	1.29 (0.03)	189 (9)	11 (1)	74 (3)	40 (2)
10% MD-RBP	5420 (140)	1.23 (0.04)	305 (13)	18 (1)	152 (6)	83 (5)
10% CM-MD-RBP	5363 (180)	1.21 (0.04)	490 (32)	29 (2)	326 (29)	178 (17)
20% RBP	5430 (193)	1.23 (0.05)	389 (38)	23 (2)	194 (17)	106 (10)
20% CM-RBP	6003 (92)	1.36 (0.03)	653 (53)	39 (3)	376 (27)	205 (17)
20% MD-RBP	6297 (166)	1.43 (0.04)	911 (54)	54 (3)	519 (24)	283 (18)
20% CM-MD-RBP	6683 (146)	1.51 (0.04)	1302 (26)	78 (2)	983 (12)	536 (23)
30% RBP	6150 (210)	1.39 (0.05)	829 (44)	49 (3)	496 (33)	270 (21)
30% CM-RBP	7760 (185)	1.76 (0.05)	1532 (115)	91 (7)	1003 (57)	547 (39)
30% MD-RBP	6953 (150)	1.57 (0.04)	1775 (144)	106 (9)	1210 (68)	660 (46)
30% CM-MD-RBP	7263 (446)	1.64 (0.10)	1850 (152)	110 (9)	1590 (160)	867 (95)

All values are the average for three samples with standard deviation (in parentheses)

[a] The reinforcement factor (RF) was calculated by dividing the storage modulus for each composite by the storage modulus of the neat PVAc, i.e. the RF is the number of times the storage modulus was increased by the presence of the fibrils

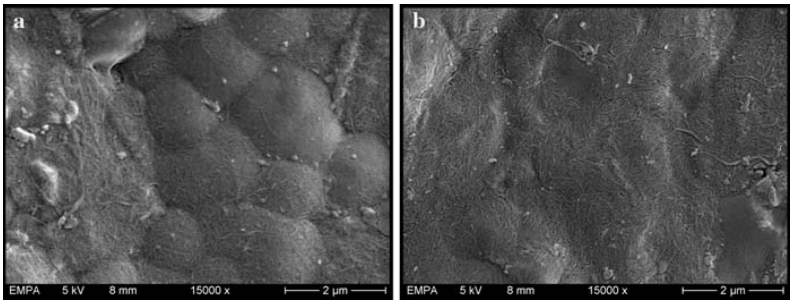

Fig. 4 FE-SEM surfaces of PVAc nanocomposites with 10(**a**) and 30 (**b**) wt% of the CM-MD-RBP cellulose fibrils

fibril aggregates that were not completely refined during the chemical and mechanical treatments.

When considering all nanocomposites at any given fibril content, those prepared with the CM-MD-RBP nanofibrils clearly showed the highest RF values at 80 and 150 °C followed by the MD-RBP, CM-RBP and the untreated RBP fibrils. Differences between the treatments were maximum at lower contents and decreased when the fibril contents increased. These differences between the treatments might be

explained because mechanical disintegration of the RBP (MD-RBP) breaks down the RBP fibrous material into thinner parts providing cellulose nanofibrils with higher aspect ratio, and consequently, with higher reinforcing potential (Chakraborty et al. 2006). On the other hand, carboxymethylation of the RBP nanofibers (CM-RBP) increases the degree of swelling of the fibers and opens up the fiber structure (Walecka 1956), facilitating not only fiber/fiber and fiber/matrix interactions but also further microfibrilation (CM-MD-RBP) (Wågberg et al. 2008). In fact, a synergistic effect between the treatments was found at 5 and 10 wt% and 5, 10 and 20 wt% fibril loadings at 80 and 150 °C, respectively. This is shown by a synergy ratio, defined as the RF provided by the cellulose nanofibrils that were first chemically modified and subsequently mechanically disintegrated (CM-MD-RBP) divided by the sum of the individual RFs due to the fibrils that were chemically (CM-RBP) and the fibrils that were mechanically modified (MD-RBP), greater than 1 for these compositions (Table 4). As expected, this synergistic effect was more significant for nanocomposites prepared with the lowest fibril content (5 wt%) with ratios around 1.6 (80 °C) and 2.2 (150 °C), suggesting that the CM-MD-RBP nanofibrils form the most effective percolating network within the PVOH matrix. As the fibril content increased, the synergistic effect was progressively reduced and it vanished for nanocomposites with 20 and 30 wt% at 80 °C and for nanocomposites with 30 wt% at 150 °C (ratio < 1). Consequently, from an economical point of view, the extra cost in treating and obtaining the CM-MD-RBP fibrils might limit their use to low concentrations, whereas at high concentrations (e.g. 30 wt%) the MD-RBP fibrils (RF of 1208 at 150 °C), the CM-RBP (RF of 1001 at 150 °C) or even the untreated RBP (RF of 494 at 150 °C) might be a better choice than the CM-MD-RBP (RF of 1588 at 150 °C).

Table 4 Synergistic effects between treatments at 80 and 150 °C

Fibril content (%)	Synergy ratio[a]	
	80 °C	150 °C
5	1.56 (0.07)	2.23 (0.06)
10	1.01 (0.07)	1.44 (0.13)
20	0.83 (0.04)	1.10 (0.05)
30	0.56 (0.06)	0.72 (0.08)

All values are the average for three samples with standard deviation (in parentheses)

[a] The synergy ratio is defined as the ratio of the reinforcement factor (RF) due to the fibrils that were chemically modified followed by mechanical disintegration (CM-MD-RBP, treatments acting together) divided by the sum of the individual RFs due to the fibrils that were chemically (CM-RBP) and the fibrils that were mechanically modified (MD-RBP) at the same concentration. A ratio higher than 1 implies a synergistic effect

Considering the outstanding reinforcing potential provided by the studied cellulose fibrils to the PVAc latex adhesive in the high temperature region, a preliminary study on their suitability to prepare wood adhesives to manufacture beech bonded assemblies with higher heat resistance was conducted. Therefore, three adhesive formulations, namely, the neat PVAc and the PVAc with 1 and 3 wt% of the CM-RBP were employed to prepare boards as previously described (Table 1). The CM-RBP fibrils were chosen for this study, regardless of the lower reinforcing potential respect to the MD-RBP and CM-MD-RBP (both obtained as aqueous suspensions), because they were obtained in powder form (but easily redispersible in water). Therefore, the CM-RBP fibrils are not only more stable (especially against bacterial decomposition) allowing significant savings in storage and, consequently, in shipping, but also they facilitate the preparation of wood adhesives with a tailored solids content and a better control of the viscosity prior to wood bonding. In particular, the addition of the CM-RBP fibrils to the neat PVAc latex led to a more pseudoplastic behaviour of the resulting adhesives as the power law index (n) decreased from 0.74 to 0.41 (Fig. 1). This behavior is of great interest because, as the adhesive is subjected to stress during its application, its apparent viscosity will decrease, resulting in better flow, and consequently enhancing the spreading of the adhesive over the wood surface.

Table 5 shows the average shear strength with standard deviation for the three boards after the conditioning treatments (Table 2). As it can be observed, all boards easily met the requirement for durability class D1 (dry shear strength > 10 N/mm^2). However, one-way ANOVA showed that the addition of fibrils had a detrimental effect on the shear strength of the boards ($p < 0.05$) when tested in dry conditions, and both boards prepared with 1 and 3% of CM-RBP fibrils showed significantly lower shear strengths than the neat PVAc. When the requirement for

Table 5 Average shear strength values with standard deviation for boards 1–3 after the conditioning treatments (see Table 2 for details)

Board	Adhesive	Shear strength (N/mm^2)		
		Durability class D1[1]	Durability class D3[1]	WATT 91[1]
1	Neat PVAc	19.4 ± 2.8^{a}	1.7 ± 0.3^{a}	4.6 ± 0.6^{a}
2	PVAc-1% CM-RBP	14.7 ± 0.6^{b}	1.4 ± 0.2^{b}	5.1 ± 0.7^{a}
3	PVAc-3% CM-RBP	14.8 ± 1.1^{b}	$1.5 \pm 0.2^{a,b}$	5.9 ± 0.4^{b}

One-way analysis of variance was performed on the shear strength data for each treatment

[1] For each treatment, same letter indicates that the shear strength data is not significantly different

durability class D3 (wet shear strength > 2 N/mm^2) was tested, surprisingly, none of the boards prepared passed the test. This was unexpected, since the commercial neat PVAc used in this study was classified as suitable for durability class D3 by the provider. Again, one-way ANOVA showed that the addition of fibrils had an adverse effect on the properties of the boards ($p < 0.05$). However, in this case, the average shear strength value for the board with 3 wt% of CM-RBP fibrils was not significantly different than that of the neat PVAc adhesive. Finally, when tested in the WATT 91 test (briefly, lap joint specimens tested after 1 h at 80 °C), addition of the fibrils also had a significant effect (one-way ANOVA, $p < 0.05$) but in this case, positive, since the board reinforced with 3 wt% of fibrils showed a significantly higher shear strength value than the control sample. This indicates a significant increase in heat resistance when using the PVAc adhesive reinforced with 3 wt% fibrils and it is in agreement with the reinforcing effect observed in Table 3 (DMA data) at 80 °C for all nanocomposites containing the CM-RBP fibrils. The observed decrease in adhesion (durability class D1) might be associated to the reduction in apparent viscosity induced by the fibrils (the neat PVAc apparent viscosity was approx. three times higher than those for the adhesives containing the fibrils). This, while improving spreadability, might also result in an increased penetration of the fibril-containing adhesives into the wood which in turn could lead to a weaker glue line. In addition, the presence of the cellulose nanofibrils might also perturb the film forming process of PVAc negatively affecting adhesion. On the other hand, the fact that carboxymethylated cellulose fibrils are quite hydrophilic and consequently, more accessible to water might explain the reduction in durability. Finally, in agreement with the DMA data, the presence of the fibrils is stiffening the glue line which while not contributing to improve adhesion at room temperature, becomes essential when tested at 80 °C. Collectively, these results indicated that the addition of the carboxymethylated fibrils (CM-RBP) to a PVAc latex effectively enhanced the heat resistance of the glue line of beech bonded assemblies but generally reduced its performance under dry (durability class D1) and wet conditions (durability class D3). Further studies will be conducted to optimize the main parameters involved in the PVAc preparation (e.g. solids content, viscosity, cellulose fibril content, other type of cellulose fibrils, other type of PVAc latex, etc.) in an attempt to prepare adhesive formulations that will also fulfill the durability class D3 and WATT 91 requirements.

Conclusions

The untreated and processed cellulose nanofibrils used in this work had a remarkable influence on the viscoelastic properties of PVAc latex films as demonstrated by significant increases in storage modulus in the whole temperature range and by significant decreases in tan δ above the glassy state. This was mainly attributed to a strong interaction between the cellulose nanofibrils network and the highly hydrophilic PVOH matrix that dramatically restricted segmental motions of the PVOH chains. Among the different cellulose nanofibrils at any given concentration in the high temperature region, those that were carboxymethylated and subsequently mechanically disintegrated provided the largest reinforcement followed by those that were only mechanically disintegrated, those that were only carboxymethylated, and the untreated ones. However, the higher technical and

energetic operating expenses necessary to produce the CM-MD-RBP fibrils might only be justifiable when they are used at very low contents (5 wt%), where the difference in reinforcement respect to the other types of fibrils is maximum. Otherwise, the simple mechanical treatment seems a better choice since the resulting fibrils not only provide a large reinforcement at a smaller processing cost but also they are less hydrophilic than the carboxymethylated fibrils and therefore less accessible to water. This proved important when the CM-RBP fibrils were used to prepare adhesives, since boards prepared with this type of fibrils clearly passed the test for durability class D1 and showed significantly enhanced heat resistance (EN 14257), but failed the test for durability class D3.

Collectively, these findings are encouraging to conduct a more thorough study with the other types of fibrils, especially the MD-RBP, and PVAc latexes so that the durability class 3 and specific heat resistance requirements (e.g. for windows sections the shear strength > 7 N/mm^2) are met.

Acknowledgments The authors would like to thank Mr. Daniel Heer, Mr. Walter Risi and Mr. Michael Strässle (Wood Lab, Empa) for their technical assistance in the manufacture, ageing and testing treatments, respectively, of the bonded assemblies.

References

Alemdar A, Sain M (2008) Biocomposites from wheat straw nanofibers: morphology, thermal and mechanical properties. Compos Sci Technol 68(2):557–565

Andresen M, Johansson LS, Tanem BS, Stenius P (2006) Properties and characterization of hydrophobized microfibrillated cellulose. Cellulose 13:665–677

Araki J, Wada M, Kuga S (2001) Steric stabilization of a cellulose microcrystal suspension by poly(ethylene glycol) grafting. Langmuir 17:21–27

Azizi Samir MAS, Alloin F, Dufresne A (2005) Review of recent research into cellulosic whiskers, their properties and their application in nanocomposite field. Biomacromolecules 6:612–626

Backman AC, Lindberg KAH (2004) Interaction between wood and polyvinyl acetate glue studied with dynamic mechanical analysis and scanning electron microscopy. J Appl Polym Sci 91:3009–3015

Bordeanu N, Eyholzer C, Zimmermann T (2008) Cellulose nanostructures with tailored functionalities. Pending patent

Cantiani R, Guerin G, Senechal A, Vincent I, Benchimol J (2001a) Supplementation of cellulose nanofibrils with carboxycellulose with low degree of substitution. US patent 6231657

Cantiani R, Guerin G, Senechal A, Vincent I, Benchimol J (2001b) Additivation of essentially amorphous cellulose nanofibrils with carboxyl cellulose with a high degree of substitution. US patent 6224663

Cantiani R, Guerin G, Senechal A, Vincent I, Benchimol J (2001c) Supplementation of essentially amorphous cellulose nanofibrils with carboxycellulose which has a high degree of substitution. US patent 6306207

Cash MJ, Chan AN, Conner HT, Cowan PJ, Gelman RA, Lusvardi KM, Thompson SA, Tise FP (2000) Derivatized microfibrillar polysaccharide. WO patent 0047628

Chakraborty A, Sain M, Kortschot M (2006) Reinforcing potential of wood pulp-derived microfibres in a PVA matrix. Holzforschung 60:53–58

Couderc S, Ducloux O, Kim BJ, Someya T (2009) A mechanical switch device made of a polyimide-coated microfibrillated cellulose sheet. J Micromech Microeng 19:055006

Dalmas F, Cavaillé JY, Gauthier C, Chazeau L, Dendievel R (2007) Viscoelastic behaviour and electrical properties of flexible nanofiber filled polymer nanocomposites. Influence of procesing conditions. Comp Sci Technol 67:829–839

De Rodriguez NLG, Thielemans W, Dufresne A (2006) Sisal cellulose whiskers reinforced polyvinyl acetate nanocomposites. Cellulose 13(3):261–270

Dinand E, Chanzy H, Vignon MR, Maureaux A, Vincent I (1996) Microfibrillated cellulose and method for preparing same from primary wall plant pulp, particularly sugar beet pulp. WO patent 9624720

European Standard EN 14257:2006 Adhesives—wood adhesives—determination of tensile strength of lap joints at elevated temperature (WATT'91)

European Standard EN 204:2001 Classification of thermoplastic wood adhesives for non-structural applications

European Standard EN 205:2003 Adhesives—wood adhesives for non-structural applications—determination of tensile shear strength of lap joints

Excoffier G, Vignon M, Benchimol J, Vincent I, Hannuskela T, Chauve V (1999) Parenchyma cellulose substituted with carboxyalkyl groups and preparation method. WO patent 9938892

Eyholzer C, Bordeanu N, Lopez-Suevos F, Rentsch D, Zimmermann T, Oksman K (2009) Preparation and characterization of water-redispersible nanofibrillated cellulose in powder form. Cellulose, under final revision

Eyler RW, Klug ED, Diephuis F (1947) Determination of degree of substitution of sodium carboxymethylcellulose. Anal Chem 19(1):24–27

Goussé C, Chanzy H, Cerrada ML, Fleury E (2004) Surface silylation of cellulose microfibrils: preparation and rheological properties. Polymer 45:1569–1575

Herrick FW (1984) Process for preparing microfibrillated cellulose. US patent 4481077

Hubbe MA, Rojas OJ, Lucia LA, Sain M (2008) Cellulosic nanocomposites: a review. BioRes 3(3):929–980

Hult EL, Larsson PT, Iversen T (2001) Cellulose fibril aggregation—an inherent property of kraft pulps. Polymer 42:3309–3314

Iwamoto S, Nakagaito AN, Yano H (2007) Nano-fibrillation of pulp fibers for the processing of transparent nanocomposites. Appl Phys A: Mater Sci Process 89(2):461–466

Kristo E, Biliaderis CG (2007) Physical properties of starch nanocrystal-reinforced pullulan films. Carbohyd Polym 68:146–158

Kvien K, Oksman K (2007) Orientiation of cellulose nanowhiskers in polyvinyl alcohol. Appl Phys A 87:641–643

Laivins GV, Scallan AM (1993) The mechanism of hornification of wood pulps. In: Baker CF (ed) Products of papermaking. Trans. 10th fundamental research symposium. Pira International, Oxford, pp 1235–1260

Lasseuguette E (2008) Grafting onto microfibrils of native cellulose. Cellulose 15:571–580

Lindström T, Carlsson G (1982) The effect of carboxyl groups and their ionic form during drying on the hornification of cellulose fibers. Svensk Papperstidn 85(15):R146–R151

López-Suevos F, Frazier CE (2005) Parallel-plate rheology of latex films bonded to wood. Holzforschung 59:435–440

López-Suevos F, Frazier CE (2006) The role of resol fortifiers in latex wood adhesives. Holzforschung 60:561–566

Lu J, Wang T, Drzal LT (2008) Preparation and properties of microfibrillated cellulose polyvinyl alcohol composite materials. Compos Part A-Appl S 39(5):738–746

Nakagaito AN, Yano H (2004) The effect of morphological changes from pulp fiber towards nano-scale fibrillated cellulose on the mechanical properties of high-strength plant fiber based composites. Appl Phys A: Mater Sci Process 78(4):547–552

Nakagaito AN, Yano H (2005) Novel high-strength biocomposites based on microfibrillated cellulose having nano-order-unit web-like network structure. Appl Phys A: Mater Sci Process 80(1):155–159

Nakagaito AN, Yano H (2008) The effect of fiber content on the mechanical and thermal expansion properties of biocomposites based on microfibrillated cellulose. Cellulose 15(4):555–559

Roohani M, Habibi Y, Belgacem NM, Ebrahim G, Karimi AN, Dufresne A (2008) Cellulose whiskers reinforced polyvinyl alcohol copolymers nanocomposites. Eur Polym J 44(8):2489–2498

Saito T, Nishiyama Y, Putaux JL, Vignon M, Isogai A (2006) Homogeneous suspensions of individualized microfibrils from TEMPO-catalyzed oxidation of native cellulose. Biomacromolecules 7:1687–1691

Samir M, Alloin F, Paillet M, Dufresne A (2004) Tangling effect in fibrillated cellulose reinforced nanocomposites. Macromolecules 37(11):4313–4316

Sassi JF, Chanzy H (1995) Ultrastructural aspects of the acetylation of cellulose. Cellulose 2:111–127

Stenstad P, Andresen M, Tanem BS, Stenius P (2008) Chemical surface modifications of microfibrillated cellulose. Cellulose 15:35–45

Wågberg L, Decher G, Norgren M, Lindstrom T, Ankerfors M, Axnas K (2008) The build-up of polyelectrolyte multilayers of microfibrillated cellulose and cationic polyelectrolytes. Langmuir 24:784–795

Walecka JA (1956) An investigation of low degree of substitution carboxymethylcelluloses. Tappi 39(7):458–463

Yano H, Nakahara S (2004) Bio-composites produced from plant microfiber bundles with a nanometer unit web-like network. J Mater Sci 39:1635–1638

Yano H, Sugiyama J, Nakagaito AN, Nogi M, Matsuura T, Hikita M, Handa K (2005) Optically transparent composites reinforced with networks of bacterial nanofibers. Adv Mater 17:153–155

Young RA (1994) Comparison of the properties of chemical cellulose pulps. Cellulose 1:107–130

Zadorecki P, Michell AJ (1989) Future-prospects for wood cellulose as reinforcement in organic polymer composites. Polym Compos 10:69–77

Zimmermann T, Pöhler E, Geiger T (2004) Cellulose fibrils for polymer reinforcement. Adv Eng Mat 6(9):754–761

Zimmermann T, Pöhler E, Schwaller P (2005) Mechanical and morphological properties of cellulose fibril reinforced nanocomposites. Adv Eng Mater 7(12):1156–1161

Paper III

Cellulose
DOI 10.1007/s10570-010-9423-9

Reinforcing effect of carboxymethylated nanofibrillated cellulose powder on hydroxypropyl cellulose

Ch. Eyholzer · F. Lopez-Suevos · P. Tingaut · T. Zimmermann · K. Oksman

Received: 8 March 2010 / Accepted: 26 April 2010

Abstract Bionanocomposites of hydroxypropyl cellulose (HPC) and nanofibrillated cellulose (NFC) were prepared by solution casting. The various NFC were in form of powders and were prepared from refined, bleached beech pulp (RBP) by mechanical disintegration, optionally combined with a pre- or post mechanical carboxymethylation. Dynamic mechanical analysis (DMA) and tensile tests were performed to compare the reinforcing effects of the NFC powders to those of their never-dried analogues. For unmodified NFC powders an inferior reinforcing potential in HPC was observed that was ascribed to severe hornification and reagglomeration of NFC. In contrast, the composites with carboxymethylated NFC showed similar behaviors, regardless of the NFC suspensions being dried or not prior to composite preparation. SEM characterization confirmed a homogeneous dispersion of dried, carboxymethylated NFC within the HPC matrix. These results clearly demonstrate that drying of carboxymethylated NFC to a powder does not decrease its reinforcing potential in (bio)nanocomposites.

Keywords Nanofibrillated cellulose · Hydroxypropyl cellulose · Hornification · Nanocomposites · Morphology · Dynamic mechanical properties · Mechanical properties

Ch. Eyholzer (✉) · F. Lopez-Suevos · P. Tingaut · T. Zimmermann
Swiss Federal Laboratories for Materials Science and Technology (Empa), Dübendorf, Switzerland
e-mail: christian.eyholzer@empa.ch

Ch. Eyholzer · K. Oksman
Division of Manufacturing and Design of Wood and Bionanocomposites, Luleå University of Technology (LTU), Luleå, Sweden

F. Lopez-Suevos
Centro de Innovación e Servizos Tecnolóxicos da Madeira de Galicia, CIS-Madeira, Parque Tecnolóxico de Galicia, Galicia, Spain

Introduction

The general awareness of the increasing need for environmentally benign materials in building and construction, automotive and packaging at low cost has promoted a drastic increase in the research activities towards composites based on renewable and sustainable plant fibers (Hubbe et al. 2008). Among all biopolymers, cellulose is the most abundant and combines high strength and stiffness with low density and biodegradability (Zadorecki and Michell 1989; Couderc et al. 2009). Its inherent mechanical properties arise from β-1,4 linked glucopyranose chains, aligned into highly ordered (crystalline) domains by intra- and intermolecular hydrogen bonds. These crystallites are linked by amorphous domains to form bundles of fibrils (Azizi Samir et al. 2005).

Published online: 08 May 2010

Successful isolation of cellulose fibrils with diameters below 100 nm is usually done by applying high shear forces to an aqueous suspension of never-dried cellulose pulp (Turbak et al. 1983; Herrick et al. 1983; Wågberg et al. 1987; Yano and Nakahara 2004; Zimmermann et al. 2004; Jonoobi et al. 2009). In order to enhance disintegration rate and lower energy consumption, chemical (Wågberg et al. 1987; Saito et al. 2006) and enzymatic (Pääkkö et al. 2007) pretreatments were applied. However, the yielded suspensions of nanofibrillated cellulose contain large amounts of water. Therefore, they suffer from bacterial degradation, require large storage facilities and generate high transportation costs. These ramifications could be avoided by preparing nanofibrillated cellulose (NFC) in powder form. However, simple drying of cellulose pulp from an aqueous suspension leads to irreversible agglomeration of the fibrils, called hornification (Scallan and Tigerström 1992; Laivins and Scallan 1993; Young 1994; Hult et al. 2001). This problem can be solved by functionalization of cellulose hydroxyl groups with carboxymethyl groups in their sodium form (Lindström and Carlsson 1982; Laivins and Scallan 1993). Following this approach, we recently reported the preparation and characterization of water-redispersible, chemically modified NFC powders (Eyholzer et al. 2010). The high interest in producing NFC in powder form for industrial application is reflected by several patents (Herrick 1984; Bahia 1995; Dinand et al. 1996; Excoffier et al. 1999; Cantiani et al. 2001; Cash et al. 2003; Bordeanu et al. 2008).

Nevertheless, the NFC starting material for mechanical reinforcement of polymer matrices is still predominantly used in form of never-dried aqueous suspensions. Several studies showed its high reinforcing potential on hydrophilic matrices like plasticized starch (Dufresne and Vignon 1998), poly(styrene-co-butyl acrylate) and poly(vinyl acetate) latexes (Azizi Samir et al. 2004; Dalmas et al. 2007; Lopez-Suevos et al. 2010), poly(vinyl alcohol) (Alemdar et al. 2009), polyurethane (Seydibeyoğlu and Oksman 2008), phenol–formaldehyde resin (Nakagaito and Yano 2005) and hydroxypropyl cellulose (Zimmermann et al. 2004). As compared to the neat matrices, these NFC composites essentially showed increased thermal stability, tensile strength and/or Young's Modulus. However, the preparation of composites containing water-redispersed NFC in powder form without the drawbacks of hornification has not been reported so far.

In this article, we present the elaboration and characterization of composites containing water-redispersed NFC powders and hydroxypropyl cellulose (HPC). This highly interesting cellulose derivative has been extensively analyzed regarding its ability to form liquid crystalline (LC) mesophases (Werbowyj and Gray 1976; Werbowyi and Gray 1980; Shimamura et al. 1981; Suto et al. 1982, 1986; Charlet and Gray 1987) and displays high compatibility with cellulosic nanofibers (Zimmermann et al. 2004; Johnson et al. 2009).

The aim of this work was to examine the effect of drying conventional and carboxymethylated NFC on their reinforcing potentials in HPC composites and further understand the interaction between the different phases. The composite films were characterized by dynamic mechanical analysis (DMA) and tensile testing and the results were compared to those from HPC composites containing the never-dried NFC counter-parts. Moreover, morphological characterization was done using scanning electron microscopy (SEM) to highlight the interactions at the fiber-matrix interface and confirm the interpretation of dynamic mechanical and tensile properties.

Materials and methods

Hydroxypropyl cellulose (HPC) with a molecular substitution (MS) of 3.4–4.4 and a weight-average molecular weight (M_w) of 100,000 was purchased from Sigma–Aldrich Chemie GmbH (Steinheim, Germany). The preparation of the various NFC powders is described elsewhere (Eyholzer et al. 2010). Briefly, refined bleached beech pulp (RBP) was carboxymethylated (c) and mechanically disintegrated using a high-shear laboratory homogenizer. In addition to RBP (untreated raw material), three NFC products were obtained by changing the sequence of the treatments (Fig. 1): NFC (mechanically isolated from RBP) and c-NFC and NFC-c (NFC that was carboxymethylated before and after mechanical disintegration, respectively), each yielded in the form of never-dried aqueous suspension and dry powder (after solvent exchange to isopropanol/ethanol 5:3 w/w and oven drying at 60 °C under repeated stirring).

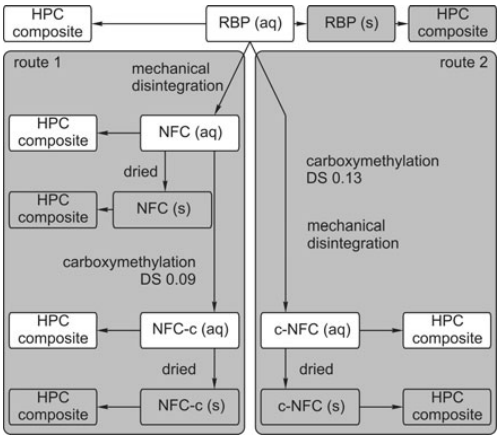

Fig. 1 Schematic overview on the sample preparation routes. In route 1 (*left block*), RBP was mechanically disintegrated (NFC), followed by carboxymethylation (NFC-c). In route 2 (*right block*), the treatments were interchanged and RBP was first carboxymethylated, followed by a mechanical disintegration step (c-NFC). White rectangles denote never-dried NFC products (aq) and composites prepared thereof. Shaded rectangles denote NFC products dried to a powder (s) and composites prepared thereof

Preparation of composite films

Composite films with fibril loadings of 5, 10 and 20% w/w were prepared at room temperature by mixing appropriate volumes of a 2.0% w/w aqueous solution of HPC with a 2.0% w/w aqueous suspension of the various RBP and NFC products, using a blender (T 25 basic, IKA-Werke, Staufen, Germany). Samples in powder form were redispersed in deionized water to yield a 2.0% w/w aqueous suspension, prior to mixing. The suspensions were then degassed under vacuum, cast in silicon moulds and placed in a laboratory hood. The films were left to dry for several days and showed thicknesses between 40 and 150 μm.

Dynamic mechanical analysis

The viscoelastic properties of the prepared films were studied by using a RS IIIa Rheometrics System Analyzer (TA Instruments, Delaware, USA) in tension mode. The composite films were cut into rectangular specimens with 6.0 mm width and 45.0 mm length and dried by storage over silica gel under vacuum for at least 3 days.

As HPC is very difficult to dry (Pizzoli et al. 1991), possibly remaining water on the samples was removed by heating to 180 °C (140 °C for neat HPC samples and 150 °C for samples containing 5% of RBP, NFC or NFC-c) at a heating rate of 4 °C/min and hold there for 2 min for equilibration. Dynamic cooling scans were performed from 180 °C (140 and 150 °C, respectively) to −30 °C at a cooling rate of 2 °C/min and a frequency of 1 Hz. The purge gas was dry air between 180 and 35 °C and gas nitrogen below 35 °C. Initial load strain and initial static force were set to 0.09% and 2.0 g, respectively. The static force was set 15% higher than the dynamic force. The upper limit for the applied load strain was set to 0.3%. Three scans were averaged for each sample. The standard deviation in the DMA results (Figs. 2 and 3) shows the good reproducibility of the measurements for the three specimens of one sample.

Tensile testing

Modulus of elasticity (MOE), nominal tensile strength (σ_{max}) and tensile strain at break (ε) were determined according to EN ISO 527-1:1996 with slight modifications. A Universal Testing System (Zwick 1474, Ulm, Germany), equipped with a 1kN load cell was used. Small dog-bone-shaped specimens were cut from the composite films using a clicker press. The specimens had an overall length of 75.0 mm, a width of 12.0 mm at the clamping zone and a width of 4.0 mm at the stretching zone. The samples were conditioned for at least 1 week at 35% relative humidity and 20 °C. Elongation of the samples was measured by optical strain detection. MOE values were determined by the slope of the linear interpolation line of the curves between 0.1 and 0.3% strain. The initial cross head speed was set to 0.5 mm/min and increased to 5 mm/min after the determination of the MOE to minimize creeping of the samples. For each sample, six replicates were measured. Of all 150 specimens measured, six replicates were rejected due to failure of the specimen within the grips or error in test procedure.

SEM characterization

The composite films were freeze-fractured in liquid nitrogen and the surfaces were sputtered with a 7.0 nm platinum coating. The samples were observed

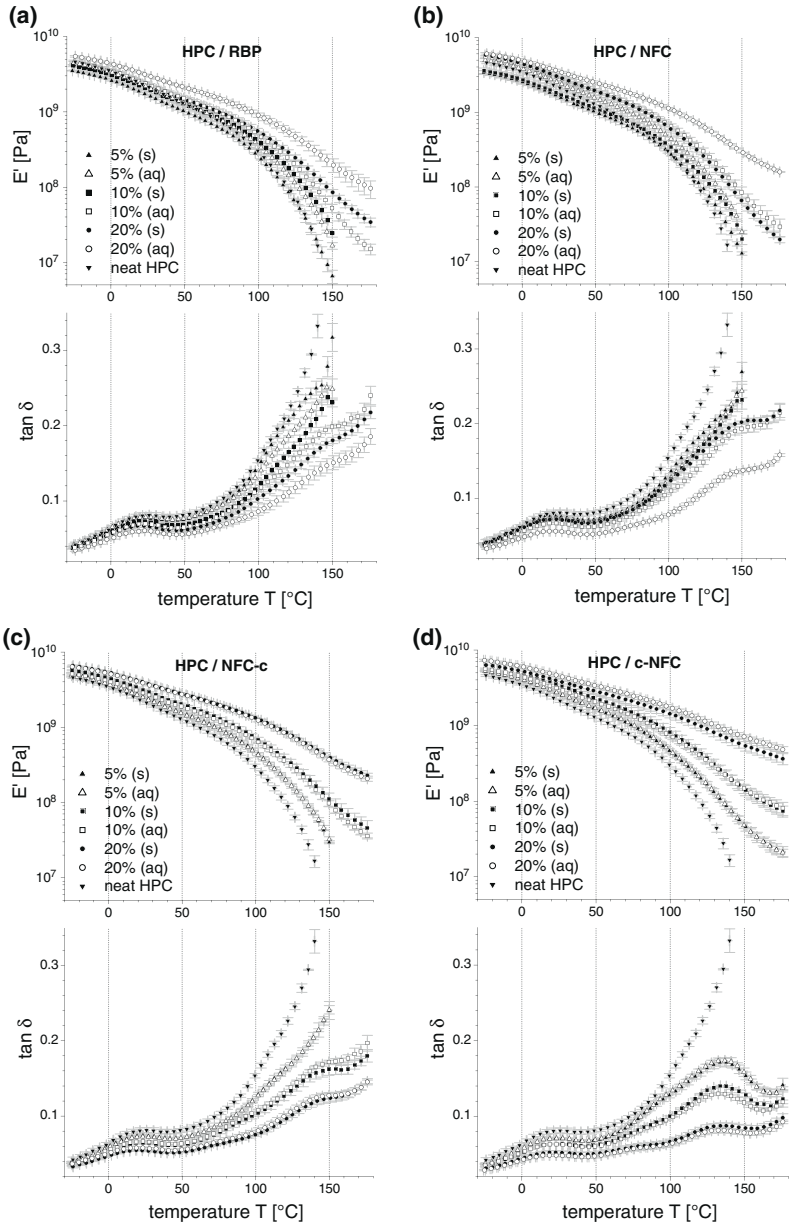

Fig. 2 Viscoelastic response of HPC films reinforced with **a** untreated RBP, **b** NFC, **c** NFC-c and **d** c-NFC. As a reference, E′ and tan delta of neat HPC films are included in all graphs

at an acceleration voltage of 5.0 kV and a working distance of 5 mm. Images were recorded in a FEI NovaNanoSEM 230 (FEI Company, Hillsboro, Oregon, USA) equipped with a Schottky field emission gun.

Results and discussion

The viscoelastic responses of all composites studied in this work are presented in Fig. 2 (with storage modulus E′ on top and tan δ below). Figure 2a shows

the viscoelastic response of HPC composite films reinforced with RBP. Figure 2b and c presents the viscoelastic response of HPC nanocomposites from route 1, containing mechanically isolated NFC and NFC that was further treated by carboxymethylation (NFC-c), respectively. Finally, Fig. 2d shows the viscoelastic response of HPC nanocomposites from route 2, containing NFC that was carboxymethylated prior to mechanical disintegration (c-NFC). Fiber loadings are marked with triangles (5% w/w), rectangles (10% w/w) and circles (20% w/w). Samples containing dried and never-dried NFC products are denoted with filled and open symbols, respectively. In all DMA graphs, the viscoelastic response of neat HPC films is included as a reference (inverted triangles). All graphs show the same temperature, storage modulus and tan δ scales in order to facilitate comparisons between nanocomposites. Also, the reproducibility of the viscoelastic response was very good, as demonstrated by the nearly perfect overlap of three repeat curves for each sample type.

Viscoelastic properties of neat HPC

The neat HPC films in Fig. 2a (inverted triangles) show three regions that are separated by two relaxations, α_a and α_m, both involving large-scale molecular motion.

In the first region, ranging from −30 to 20 °C the films exhibit a very high storage modulus which is in the range of several GPa (Pizzoli et al. 1991). At these temperatures, the bulk HPC consists of essentially three distinct phases: a crystalline phase, a disordered isotropic amorphous phase and a phase of intermediate order which was described as a frozen anisotropic amorphous phase (Rials and Glasser 1988; Pizzoli et al. 1991; Wojciechowski 2000). At 20 °C a first transition can be observed, indicated by the peak in the tan δ curve. This T_g-like transition (Aspler and Gray 1982; Rials and Glasser 1988) was attributed to the α_a relaxation, denoting a devitrification process of the disordered amorphous phase (Pizzoli et al. 1991; Wojciechowski 2000).

The second region between 20 and 130 °C is characterized by a relatively large drop in storage modulus, exhibiting a remarkable softening of the films. Around 130 °C a second T_g-like transition occurs with a strong increase in the tan δ intensity, known as the α_m relaxation (Pizzoli et al. 1991). This relaxation was explained as the transition from the frozen anisotropic phase to a mobile liquid crystal thermotropic mesophase (Pizzoli et al. 1991; Wojciechowski 2000).

In the third region above 130 °C, the storage modulus decreases drastically and the neat HPC films start to flow (Horio et al. 1988). At these temperatures, the flexible side chains of HPC act like an internal plasticizer, allowing the rather stiff main chains some mobility (Gray 1983). Due to this mobility, the main chains can orientate into a cholesteric conformation, stabilized by the side chains. Therefore, the molecular interactions of these side chains have a significant influence on the liquid crystal organization (Wojciechowski 2000). To avoid plastic deformation of the neat HPC films in tensile geometry, we limited data acquisition to 140 °C for this sample.

Viscoelastic properties of composites reinforced with never-dried (aq) NFC

To allow easier comparison, Fig. 3 shows the storage modulus values of the neat HPC films and composites with RBP and NFC products organized in columns at three arbitrary temperatures, i.e. at −20 °C (below the α_a relaxation; Fig. 3a), at 75 °C (between the α_a and α_m relaxations; Fig. 3b) and at 140 °C (above the α_m relaxation; Fig. 3c). White and dark columns denote composites containing never-dried and dried-redispersed cellulosic fillers, respectively.

As can be seen from the three diagrams, the storage modulus of the composite films increased with fiber loadings regardless of the treatment. Below the α_a relaxation at −20 °C, the increase in storage modulus was generally small (Fig. 3a). At 75 °C, after the α_a relaxation (Fig. 3b) this increase becomes more pronounced, but the strongest increase in storage modulus with higher fiber loadings compared to neat HPC was observed at 140 °C, after the α_m relaxation (Fig. 3c). This later increase in storage modulus was associated with the formation of a highly rigid percolating network of fibrils (Dalmas et al. 2007). The rigidity of this network arises from strong hydrogen bonds and entanglements between the fibrils.

Clearly, the tan δ intensity of all composites was reduced with higher filler content over the whole temperature range but most pronounced in the high

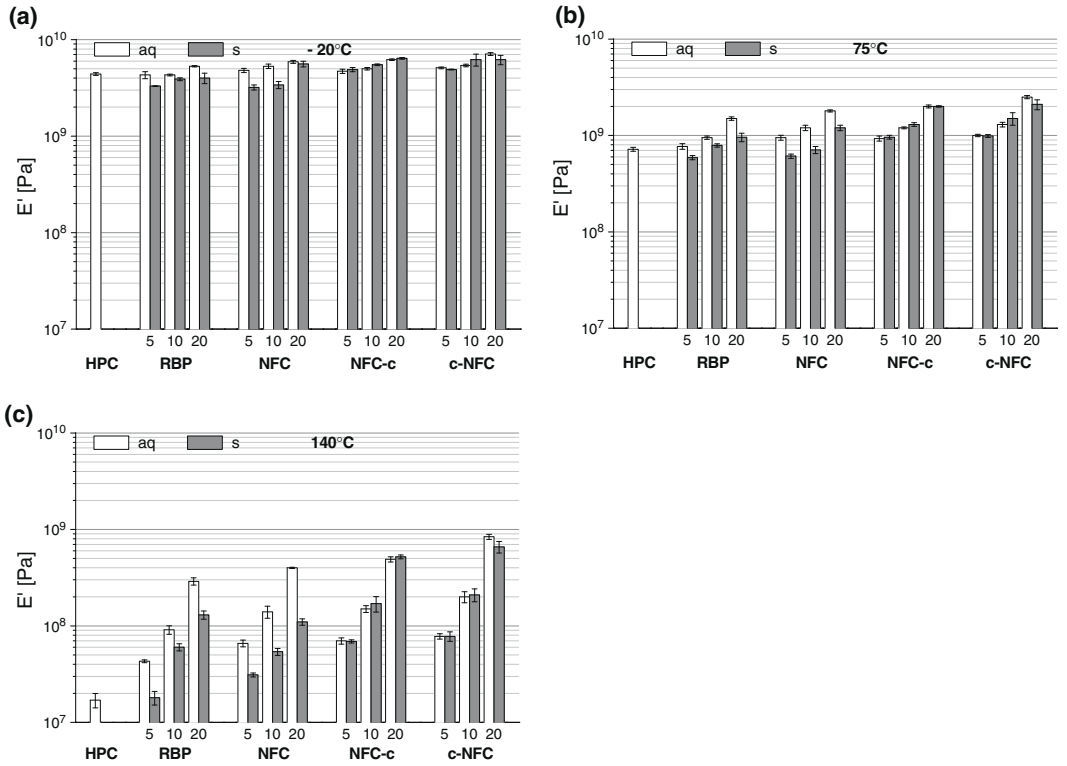

Fig. 3 Storage moduli of HPC films reinforced with RBP and NFC products at temperatures of **a** −20 °C, **b** 75 °C and **c** 140 °C. *White columns* denote films reinforced with never dried NFC products. *Dark columns* denote films reinforced with NFC products dried to a powder before compounding

temperature region above 130 °C (Fig. 2). This decrease in tan δ can (partly) be explained with the increased volume fraction of the filler in the composites. However, when comparing composites with equal loadings of filler it can be observed that the decrease in tan δ intensity depends on the filler type, becoming more pronounced in the following order: RPB < NFC < NFC-c < c-NFC (Fig. 2). This suggests that the presence of the fillers (and the percolating networks they form) promoted different degrees of segmental restrictions of the molecular motion of HPC chains, leading to an increase in E′ and a decrease in tan δ. The efficiency of these segmental restrictions may depend on surface chemistry (i.e. the availability of carboxylate groups COO^-), surface area to volume ratio and aspect ratio of the filler (Johnson et al. 2009).

It was earlier reported that carboxymethylation prior to mechanical disintegration (c-NFC) enhances the isolation of fibrils (Wågberg et al. 2008; Eyholzer et al. 2010). This might lead to the production of fibrils which are favorable in terms of the above mentioned properties compared to chemically unmodified NFC or RBP and therefore account for more efficient segmental restriction of HPC molecular motion.

Viscoelastic properties of composites reinforced with dried (s) NFC

Similarly to the composites containing the never-dried cellulosic fillers discussed above, an increase in E′ with the filler loading was observed for the composites reinforced with dried RBP and NFC,

regardless of the treatment (Fig. 3a, b and c). However, a clear difference was observed between the films containing carboxymethylated (NFC-c and c-NFC) and those containing chemically unmodified fibers (RBP and NFC). For all temperatures studied, storage modulus values of samples containing redispersed RBP and NFC were clearly lower than those of their never-dried analogues. This effect can be attributed to the hornification of RBP and NFC fibrils upon drying (Eyholzer et al. 2010), leading to a reduction of the fiber's aspect ratio and the prevention of a percolating network formation.

In contrast, films containing the dried NFC products that were carboxymethylated (NFC-c and c-NFC), showed an almost identical response as those containing the never-dried fibers in the whole temperature range (Fig. 3a, b and c). These results prove that carboxymethylated NFC can be dried and redispersed in water without affecting its mechanical performance in a nanocomposite. To confirm this suggestion, tensile tests were performed with specimens obtained from the same composite films.

Tensile tests

Figure 4a shows the nominal modulus of elasticity (MOE) of neat HPC and the composites containing RBP and NFC products in dried and never-dried condition. Once again, an increase in MOE with higher fiber loadings was measured for the films containing never-dried NFC products with a maximum increase for films containing 20% w/w of c-NFC (of up to approximately three times compared to neat HPC films).

In agreement with the data obtained from DMA, drying of carboxymethylated NFC products (NFC-c and c-NFC) did not lead to a significant reduction of the reinforcing effect, in contrast to unmodified RBP and NFC. Interestingly, films with dried NFC showed decreasing MOE values with higher loadings. Once again, this behavior was associated with an extensive hornification of the mechanically disintegrated fibrils, leading to films with poor homogeneity. The same trends were observed when analyzing the nominal strength values (σ_{max}) of the composites (Fig. 4b). Composites containing dried carboxymethylated NFC products (NFC-c and c-NFC) showed similar σ_{max} values as composites reinforced with never-dried fibers, displaying almost 3 times higher values than neat HPC. The displayed reinforcement is in the same range as observed for composites of HPC and never-dried NFC in an earlier publication (Zimmermann et al. 2004).

Figure 4c shows the strain to break values of neat HPC and the composites containing RBP and NFC products in dried and never-dried condition. Neat HPC films showed a strain to break around 20% with a relatively large standard deviation that might originate from the susceptibility of HPC towards moisture (Pizzoli et al. 1991). A clear decrease of ε was found for all composites containing chemically modified fibers (NFC-c and c-NFC), regardless of being compounded in dried or never-dried condition. This can be attributed to the rigidity of the incorporated fibrils. In agreement with the DMA results, the tensile measurements therefore confirm that carboxymethylated NFC products show the same reinforcing effect in a HPC matrix, regardless of compounded in dried or never-dried condition.

Characterization by SEM

Figure 5 shows SEM images of freeze-fractured surfaces of a neat HPC film (Fig. 5a) and composite films containing 20% w/w of dried NFC (Fig. 5b) and 20% w/w of dried c-NFC (Fig. 5c). Neat HPC showed grain sizes in the micrometer range, as already reported in the literature (Johnson et al. 2009). The composite film containing dried NFC (Fig. 5b) showed voids and large aggregations of fibrils (indicated by arrows), confirming the poor dispersion and the hornification of NFC in the matrix. In contrast, the surface morphology of composite films containing dried c-NFC was dominated by the coherent structure of the fibrils. Their orientation may suggest that the fibrils were deposited in a layered structure during the slow evaporation of water in the solution casting process. The uniform structure may origin from a homogeneous dispersion of the fibrils in the HPC matrix.

Conclusions

Bionanocomposites from hydroxypropyl cellulose (HPC) with dried and redispersed nanofibrillated cellulose (NFC) powders were prepared by solution casting from water. The various NFC powders were obtained by solely mechanical disintegration (NFC)

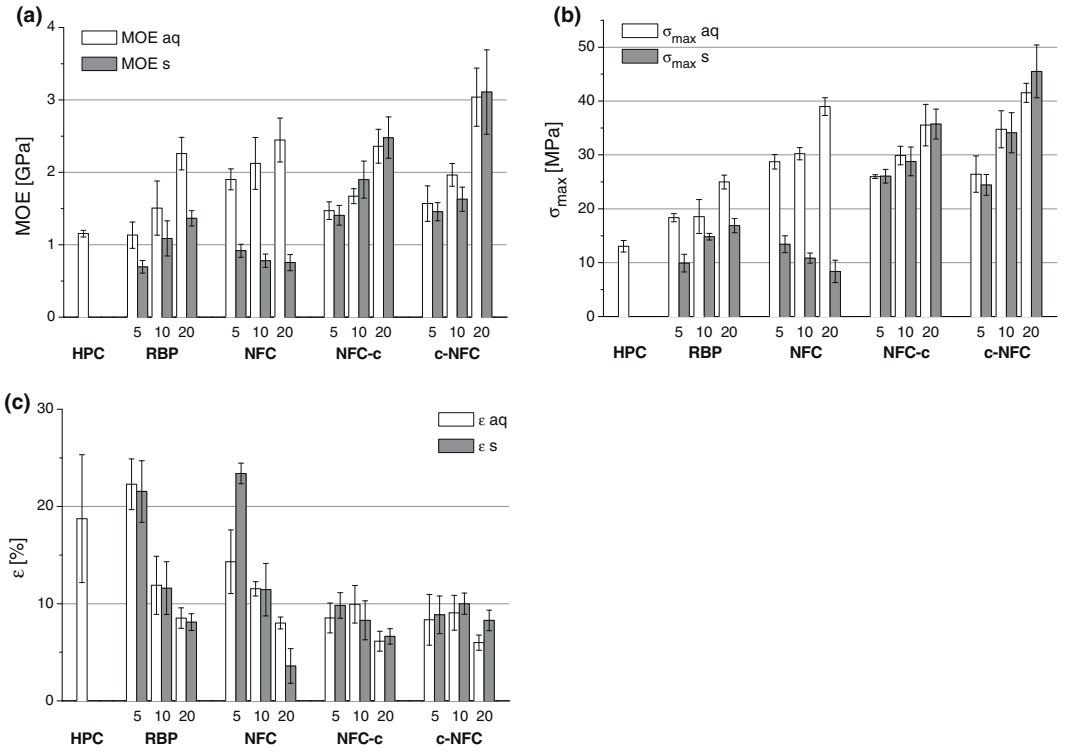

Fig. 4 **a** Modulus of elasticity, **b** ultimate strength and **c** elongation to break values of HPC films reinforced with RBP and NFC products at room temperature, obtained from tensile tests. Open columns denote films reinforced with never dried NFC products. Filled columns denote films reinforced with NFC products dried to a powder before compounding

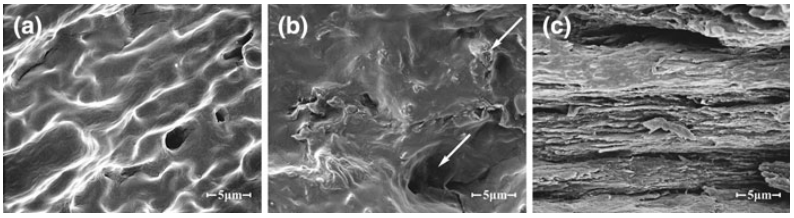

Fig. 5 SEM images of freeze-fractured surfaces from **a** neat HPC film, **b** composite film of HPC, reinforced with 20% w/w of dried and redispersed NFC and **c** composite film of HPC, reinforced with 20% w/w of dried and redispersed c-NFC. All images are magnified 10,000×

or in combination with pre- or post mechanical carboxymethylation (c-NFC and NFC-c) of refined, bleached beech pulp (RBP). The mechanical and morphological properties of the composites were analyzed by DMA, tensile tests and SEM imaging and compared to those from composites prepared with the same RBP products that were never dried.

DMA analysis and tensile tests showed that the highest reinforcing effect was observed for films containing c-NFC, in terms of storage modulus (E′), modulus of elasticity (MOE) and nominal tensile strength (σ_{max}). Enhanced isolation of the fibrils may account for the higher performance compared to the films containing the chemically unmodified RBP and

NFC fibers. In general, the mechanical response of carboxymethylated NFC products in the composites was independent of whether the fibrils were dried or not prior to compounding. NFC without carboxylate groups showed a strong decrease of its reinforcing potential when dried before mixing with HPC due to hornification. Consistently, SEM characterization of a freeze-fractured HPC film containing dried c-NFC showed a continuous and homogeneously dispersed structure.

These results demonstrate that carboxymethylated NFC preserves its mechanical reinforcing potential when dried to a powder and redispersed in water. Therefore, carboxymethylated and mechanically isolated NFC in powder form has a high potential for polymer reinforcement with increased shelf life and easier handling compared to conventional NFC aqueous suspensions.

Acknowledgments The authors gratefully acknowledge the State Secretariat for Education and Research (SER) for financial support of this work.

References

Alemdar A, Osman K, Sain M (2009) The effect of decreased fiber size in wheat straw/polyvinyl alcohol composites. J Biobased Mat Bioenerg 3:75–80

Aspler JS, Gray DG (1982) Interaction of organic vapours with hydroxypropyl cellulose. Polymer 23:43–46

Azizi Samir MAS, Alloin F, Paillet M, Dufresne A (2004) Tangling effect in fibrillated cellulose reinforced nanocomposites. Macromolecules 37:4313–4316

Azizi Samir MAS, Alloin F, Dufresne A (2005) Review of recent research into cellulosic whiskers, their properties and their application in nanocomposite field. Biomacromolecules 6:612–626

Bahia HS (1995) Treatment of cellulose. Patent publication number WO9515342

Bordeanu N, Eyholzer Ch, Zimmermann T (2008) Cellulose nanostructures with tailored functionalities. Pending patent

Cantiani R, Guerin G, Senechal A, Vincent I, Benchimol J (2001) Patent publication numbers US6224663, US6231657, US6306207

Cash MJ, Chan AN, Conner HT, Cowan PJ, Gelman RA, Lusvardi KM, Thompson SA, Tise FP (2003) Derivatized microfibrillar polysaccharide. Patent publication number WO0047628

Charlet G, Gray DG (1987) Solid cholesteric films cast from aqueous (hydroxypropyl)cellulose. Macromolecules 20: 33–38

Couderc S, Ducloux O, Kim BJ, Someya T (2009) A mechanical switch device made of a polyimide-coated microfibrillated cellulose sheet. J Micromech Microeng 19:055006

Dalmas F, Cavaillé JY, Gauthier C, Chazeau L, Dendievel R (2007) Viscoelastic behaviour and electrical properties of flexible nanofiber filled polymer nanocomposites. Influence of processing conditions. Comp Sci Technol 67: 829–839

Dinand E, Chanzy H, Vignon M, Maureaux A, Vincent I (1996) Microfibrillated cellulose and method for preparing same from primary wall plant pulp, particularly sugar beet pulp. Patent publication number WO9624720

Dufresne A, Vignon MR (1998) Improvement of starch film performances using cellulose microfibrils. Macromolecules 31:2693–2696

Excoffier G, Vignon M, Benchimol J, Vincent I, Hannuksela T, Chauve V (1999) Parenchyma cellulose substituted with carboxyalkyl groups and preparation method. Patent publication number WO9938892

Eyholzer Ch, Bordeanu N, Lopez-Suevos F, Rentsch D, Zimmermann T, Oksmann K (2010) Preparation and characterization of water-redispersible nanofibrillated cellulose in powder form. Cellulose 17:19–30

Gray DG (1983) Liquid crystalline cellulose derivatives. J Appl Polym Sci Appl Polym Symp 37:179–192

Herrick FW (1984) Process for preparing microfibrillated cellulose. Patent publication number US4481077

Herrick FW, Casebier RL, Hamilton JK, Sandberg KR (1983) Microfibrillated cellulose: morphology and accessibility. J Appl Polym Sci Appl Polym Symp 37:797–813

Horio M, Kamei E, Matsunobu K (1988) Dynamic measurements on polymer liquid crystals II. Thermotropic mesophase of hydroxypropyl cellulose. J Soc Rheol Jpn 16:27–32

Hubbe MA, Rojas OJ, Lucia LA, Sain M (2008) Cellulosic nanocomposites: a review. Biores 3:929–980

Hult EL, Larsson PT, Iversen T (2001) Cellulose fibril aggregation—an inherent property of kraft pulps. Polymer 42:3309–3314

Johnson RK, Zink-Sharp A, Renneckar SC, Glasser WG (2009) A new bio-based nanocomposite: fibrillated TEMPO-oxidized celluloses in hydroxypropylcellulose matrix. Cellulose 16:227–238

Jonoobi M, Harun J, Mathew A, Hussein M, Oksmann K (2009) Preparation of cellulose nanofibers with hydrophobic surface characteristics. Cellulose. doi: 10.1007/s10570-009-9387-9

Laivins GV, Scallan AM (1993) The mechanism of hornification of wood pulps. In: Proceedings of the 10th fundamental research symposium, Oxford, 1235–1260

Lindström T, Carlsson G (1982) The effect of carboxyl groups and their ionic form during drying on the hornification of cellulose fibers. Svensk Papperstidning 85:R146–R151

Lopez-Suevos F, Eyholzer Ch, Bordeanu N, Richter K (2010) DMA analysis and wood bonding of PVAc latex reinforced with cellulose nanofibrils. Cellulose 17:387–398

Nakagaito AN, Yano H (2005) Novel high-strength biocomposites based on microfibrillated cellulose having nano-order-unit web-like network structure. Appl Phys A 80:155–159

Pääkkö M, Ankerfors M, Kosonen H, Nykänen A, Ahola S, Österberg M, Ruokolainen J, Laine J, Larsson PT, Ikkala

O, Lindström T (2007) Enzymatic hydrolysis combined with mechanical shearing and high-pressure homogenization for nanoscale cellulose fibrils and strong gels. Biomacromolecules 8:1934–1941

Pizzoli M, Scandola M, Ceccorulli G (1991) Dielectrical and mechanical loss processes in hydroxypropylcellulose. Plast Rubber Comp Process Appl 16:239–244

Rials TG, Glasser WG (1988) Thermal and dynamic mechanical properties of hydroxypropyl cellulose films. J Appl Polym Sci 36:749–758

Saito T, Nishiyama Y, Putaux JL, Vignon M, Isogai A (2006) Homogeneous suspensions of individualized microfibrils from TEMPO-catalyzed oxidation of native cellulose. Biomacromolecules 7:1687–1691

Scallan AM, Tigerström AC (1992) Swelling and elasticity of the cell walls of pulp fibers. J Pulp Pap Sci 18:188–193

Seydibeyoğlu MO, Oksman K (2008) Novel nanocomposites based on polyurethane and micro fibrillated cellulose. Comp Sci Technol 68:908–914

Shimamura K, White JL, Fellers JF (1981) Hydroxypropylcellulose, a thermotropic liquid crystal: characteristics and structure development in continuous extrusion and melt spinning. J Appl Polym Sci 26:2165–2180

Suto S, White JL, Fellers JF (1982) A comparative study of the thermotropic mesomorphic tendencies and rheological characteristics of three cellulose derivatives: ethylene and propylene oxide esters and an acetate butyrate ester. Rheol Acta 21:62–71

Suto S, Kudo M, Karasawa M (1986) Static tensile and dynamic mechanical properties of hydroxypropylcellulose films prepared under various conditions. J Appl Polym Sci 31:1327–1341

Turbak AF, Snyder FW, Sandberg KR (1983) Microfibrillated cellulose, a new cellulose product: properties, uses, and commercial potential. J Appl Polym Sci Appl Polym Symp 37:815–823

Wågberg L, Winter L, Ödberg L, Lindström T (1987) On the charge stoichiometry upon adsorption of a cationic polyelectrolyte on cellulosic materials. Colloid Surf 27:163–173

Wågberg L, Decher G, Norgren M, Lindström T, Ankerfors M, Axns K (2008) The build-up of polyelectrolyte multilayers of microfibrillated cellulose and cationic polyelectrolytes. Langmuir 24:784–795

Werbowyi RS, Gray DG (1980) Ordered phase formation in concentrated hydroxypropylcellulose solutions. Macromolecules 13:69–73

Werbowyj RS, Gray DG (1976) Liquid crystalline structure in aqueous hydroxypropyl cellulose solutions. Mol Cryst Liq Cryst 34(Letters): 97–103

Wojciechowski P (2000) Thermotropic mesomorphism of selected (2-hydroxypropyl) cellulose derivatives. J Appl Polym Sci 76:837–844

Yano H, Nakahara S (2004) Bio-composites produced from plant microfiber bundles with a nanometer unit web-like network. J Mater Sci 39:1635–1638

Young RA (1994) Comparison of the properties of chemical cellulose pulps. Cellulose 1:107–130

Zadorecki P, Michell AJ (1989) Future-prospects for wood cellulose as reinforcement in organic polymer composites. Polym Compos 10:69–77

Zimmermann T, Pöhler E, Geiger T (2004) Cellulose fibrils for polymer reinforcement. Adv Eng Mater 6:754–761